Künstliche Intelligenz in der CT-Bildgebung

Marc Kachelrieß

German Cancer Research Center (DKFZ)
Heidelberg, Germany
www.dkfz.de/ct

Examples for

AI IN CT IMAGE FORMATION

Deep Scatter Estimation (DSE)

Network architecture & scatter estimation framework

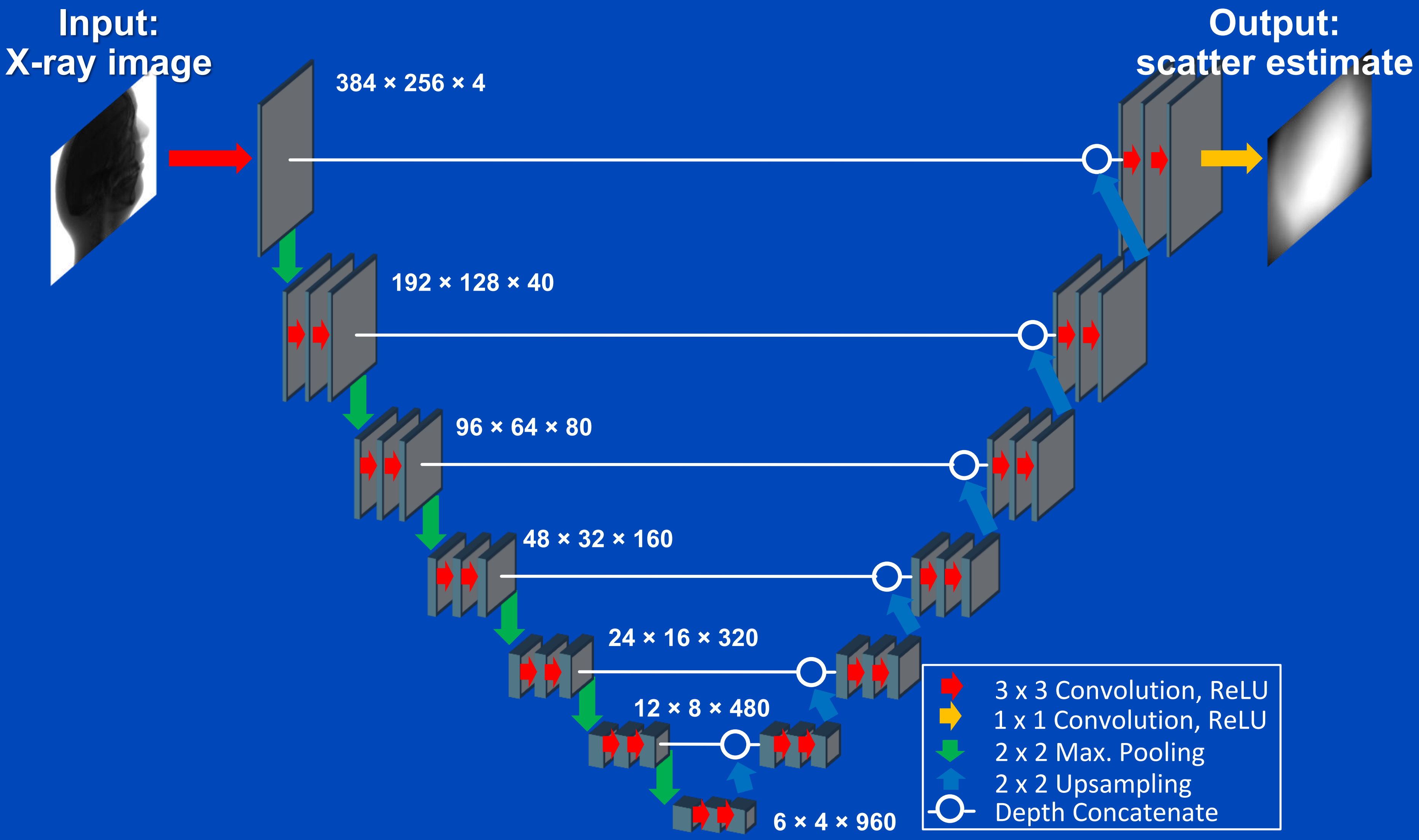

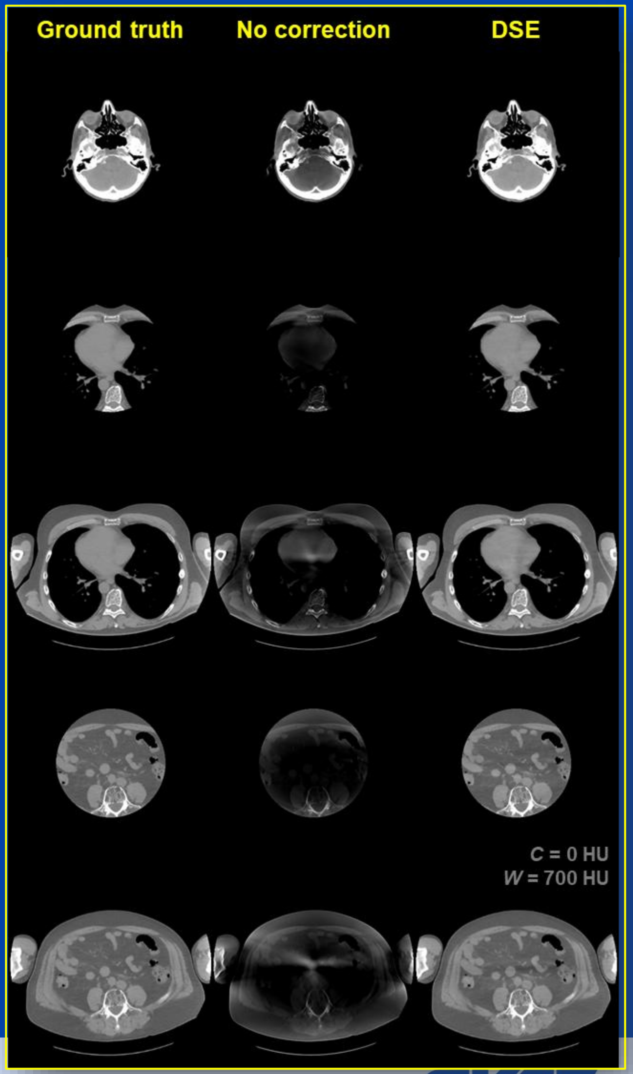

J. Maier, M. Kachelrieß et al. Deep scatter estimation (DSE). SPIE 2017 and Journal of Nondestructive Evaluation 37:57, July 2018.
J. Maier, M. Kachelrieß et al. Robustness of DSE. Med. Phys. 46(1):238-249, January 2019.

Scatter in Dual Source CT (DSCT)

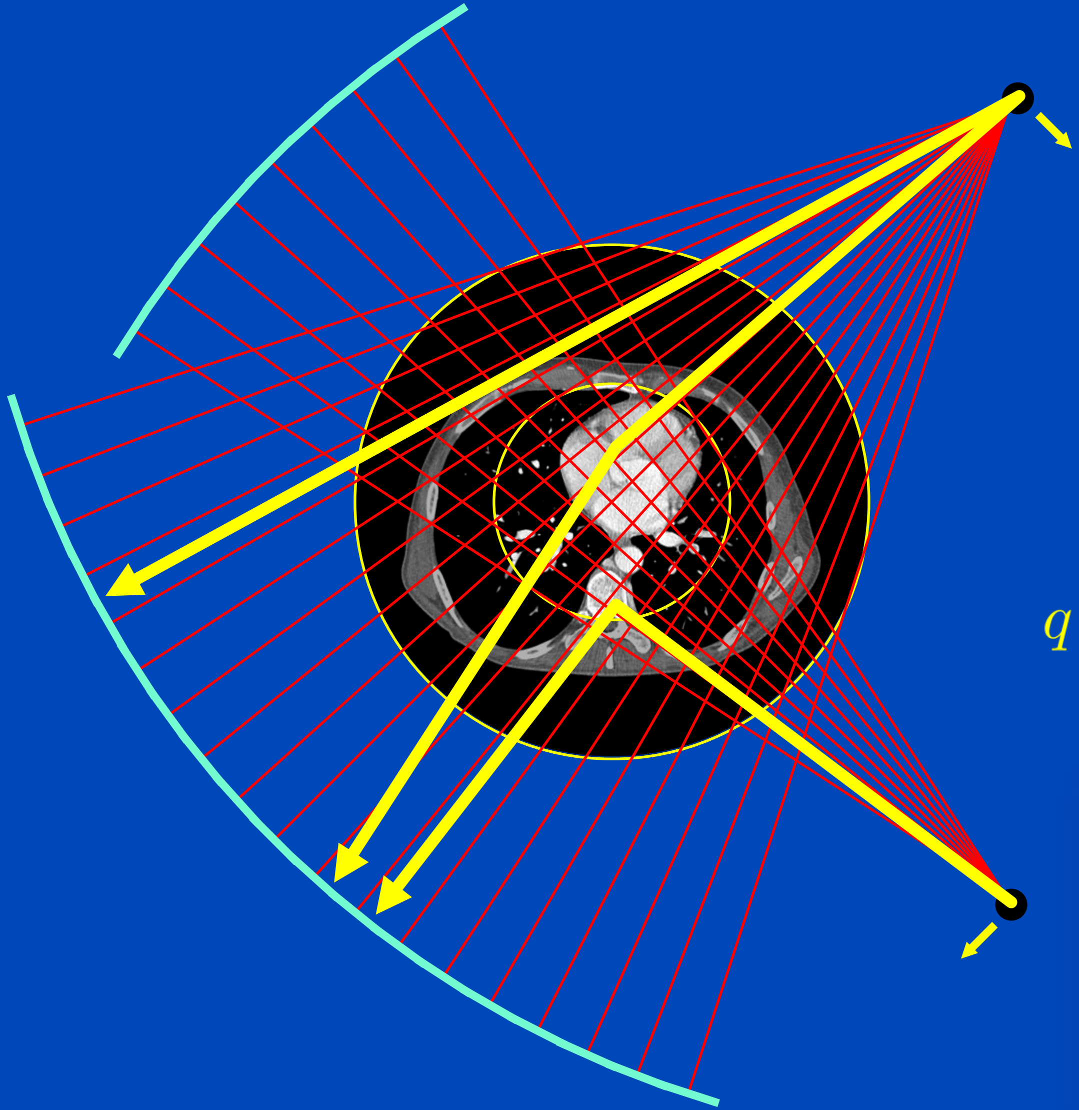

Siemens SOMATOM Force
dual source cone-beam spiral CT

$$q = -\ln \frac{I_{\text{primary}} + S_{\text{forward}} + \rho\, S_{\text{cross}}}{I_0}$$

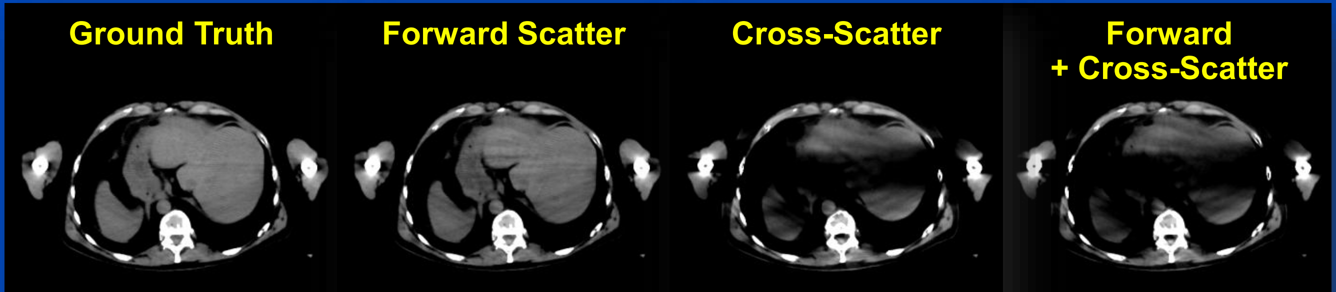

C = 40 HU, *W* = 300 HU, with 2D anti-scatter grid

J. Erath, T. Vöth, J. Maier, E. Fournié, M. Petersilka, K. Stierstorfer, and M. Kachelrieß. Deep learning-based forward and cross-scatter correction in dual source CT. Med. Phys. 48:4824–4842, July 2021.

Scatter and Cross-Scatter: DSE and Cross-DSE

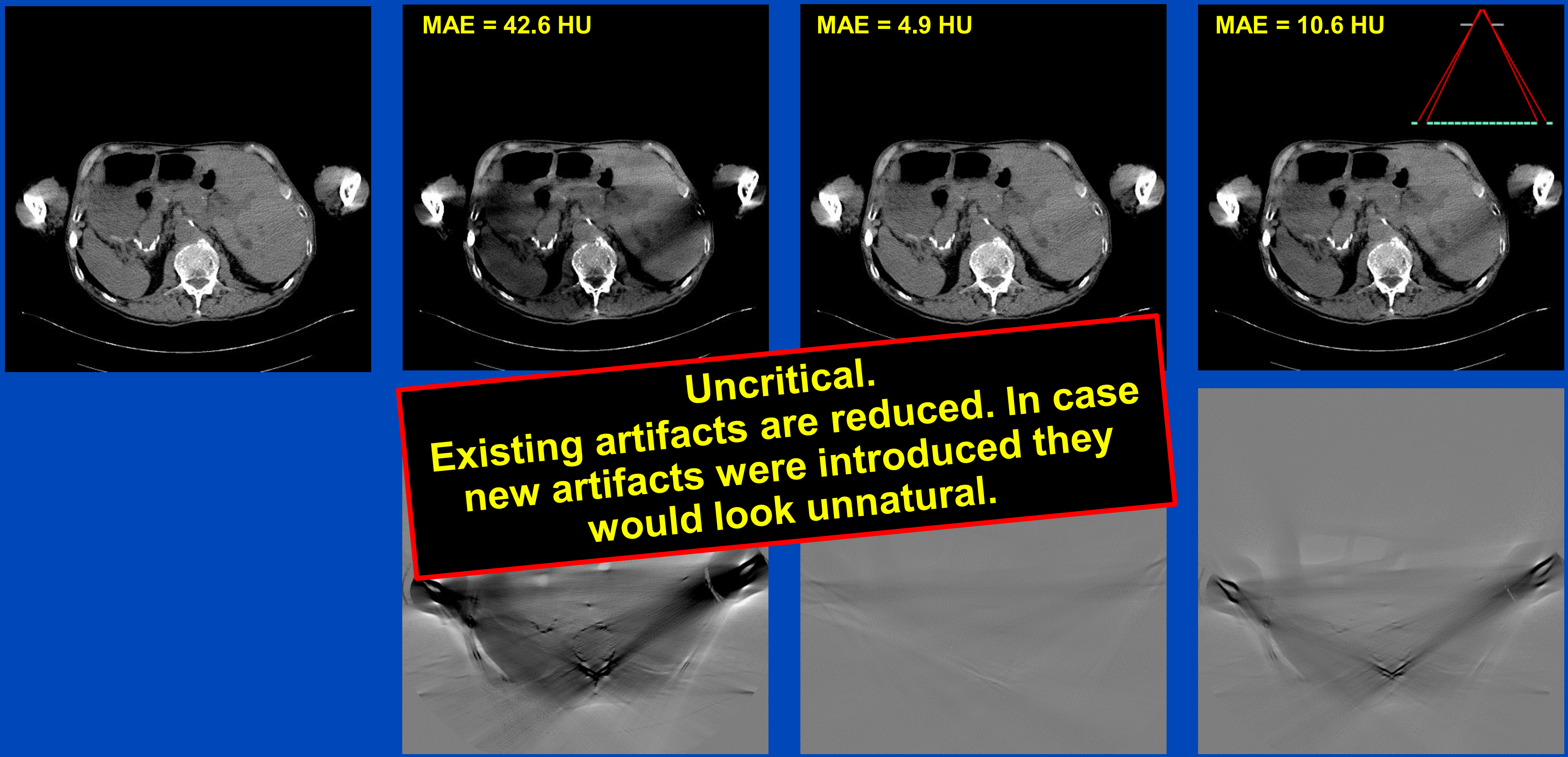

xDSE (2D, xSSE) maps

primary + forward scatter + cross-scatter + cross-scatter approximation → cross-scatter

Images C = 40 HU, W = 300 HU, difference images C = 0 HU, W = 300 HU

Canon PIQE

- Precise IQ Engine (PIQE).
- Trained on data from Canon's Precision high spatial resolution CT
- Converts images from Canon's standard spatial resolution scanners (e.g. Aquilion ONE / PRISM edition) to look like high spatial resolution images.

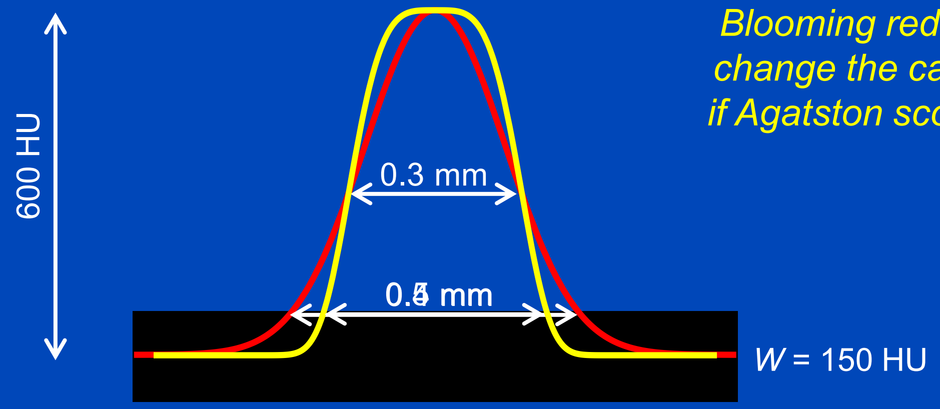

Warning:
Blooming reduction might change the calcium score, if Agatston scoring is used.

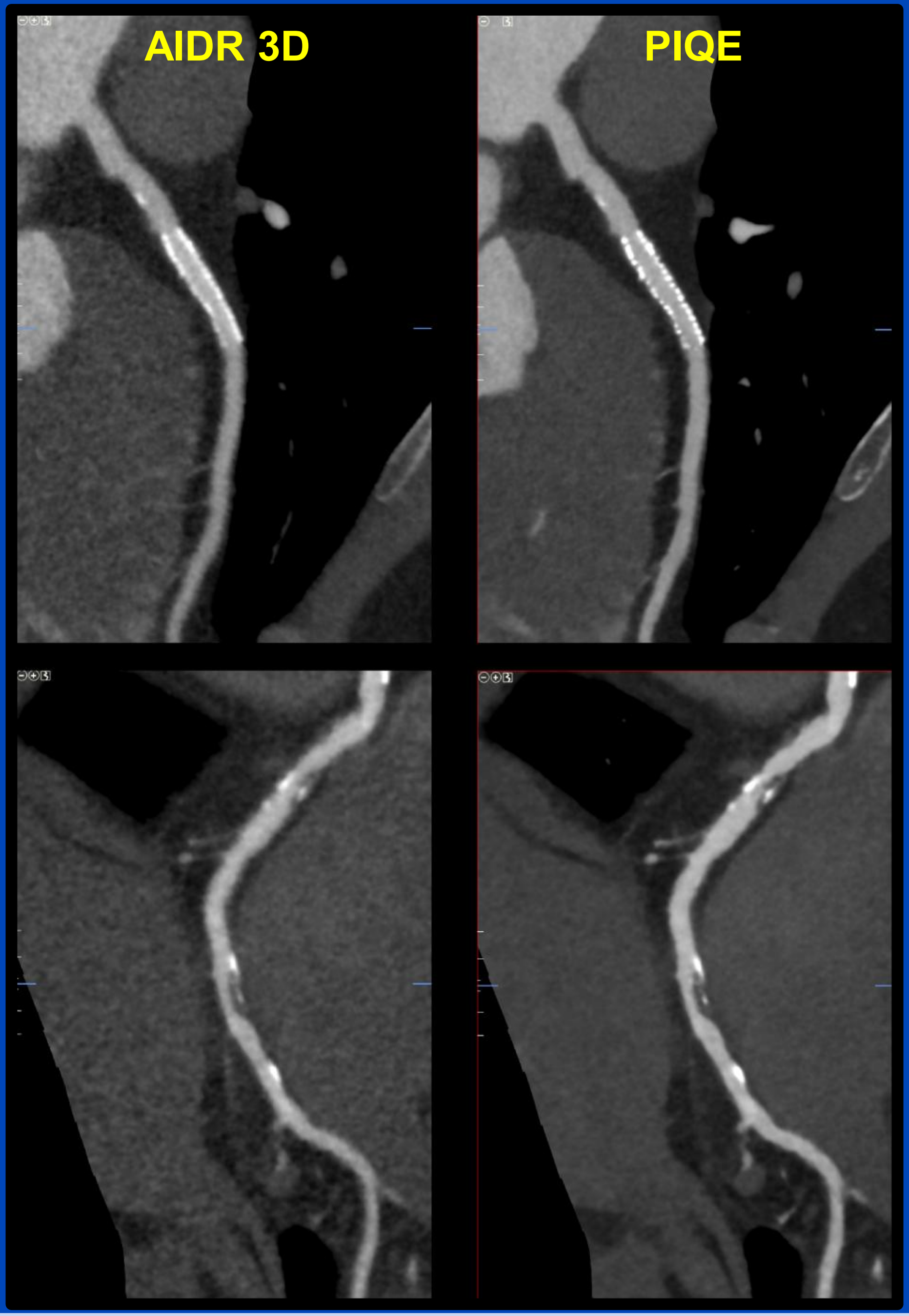

Image courtesy of Canon Medical Systems

Fake Contrast Enhancement

[1] G. Santini, L. M. Zumbo, N. Martini, G. Valvano, A. Leo, A. Ripoli, F. Avogliero, D. Chiappino, D. D. Latta, “Synthetic contrast enhancement in cardiac CT with deep learning,” arXiv 1807:01779, 2018.

[2] J. Liu, Y. Tian, A. M. Ağıldere, K. M. Haberal, M. Coşkun, C. Duzgol, and O. Akin, “DyeFreeNet: Deep virtual contrast CT synthesis,” Lecture Notes in Computer Science. Springer International Publishing, pp. 80–89, 2020.

[3] A. Chandrashekar, A. Handa, N. Shivakumar, P. Lapolla, V. Grau, R. Lee, “A deep learning approach to generate contrast-enhanced computerised tomography Angiography without the use of intravenous contrast agents,” arXiv 2003.01223, 2020.

[4] J. W. Choi, Y. J. Cho, J. Y. Ha, S. B. Lee, S. Lee, Y. H. Choi, J.-E. Cheon, and W. S. Kim, “Generating synthetic contrast enhancement from non-contrast chest computed tomography … …erative adversarial network,” Scientific Reports, vol. 11, no. 1, …

[5] S. W. Kim, J. H. Kim, S. Kwak, M. Se… …eon, “The feasibility of deep learning-based sy… …emergency department patients with acute abdo…

[6] J. Chun, J. S. Chang, C. Oh, I. Park, M… …Moon, S. Y. Chung, Y. J. Suh, and J. S. Kim, “Synthetic contra… …tomography generation using a deep convolutional neural network for cardiac substructure delineation in breast cancer radiation therapy: a feasibility study,” Radiation Oncology, vol. 17, no. 1, 2022.

[7] Y. Gao, H. Xie, C. Chang, J. Peng, S. Pan, R. L. J. Qiu, T. Wang, B. Ghavidel, J. Roper, J. Zhou, and X. Yang, “CT-based synthetic iodine map generation using conditional denoising diffusion probabilistic model,” Medical Physics, vol. 51, no. 9, pp. 6246–6258, 2024.

[8] S. Han, J.-M. Kim, J. Park, S. W. Kim, S. Park, J. Cho, S.-J. Park, H.-J. Chung, S.-M. Ham, S. J. Park, and J. H. Kim, “Clinical feasibility of deep learning based synthetic contrast-enhanced abdominal CT in patients undergoing non-enhanced CT scans,” Scientific Reports, vol. 14, no. 1, 2024.

This is a no-go.
No functional information about the vessels is measured.
All information shown is fake.

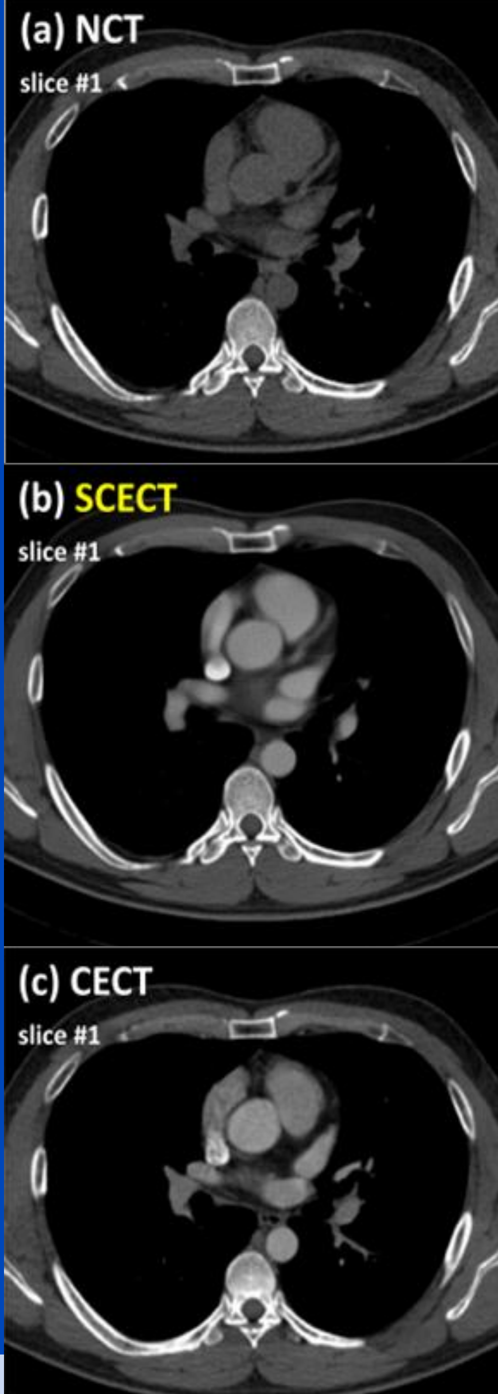

From [4]

True and Fake Spectral CT

Existing true spectral CT approaches:

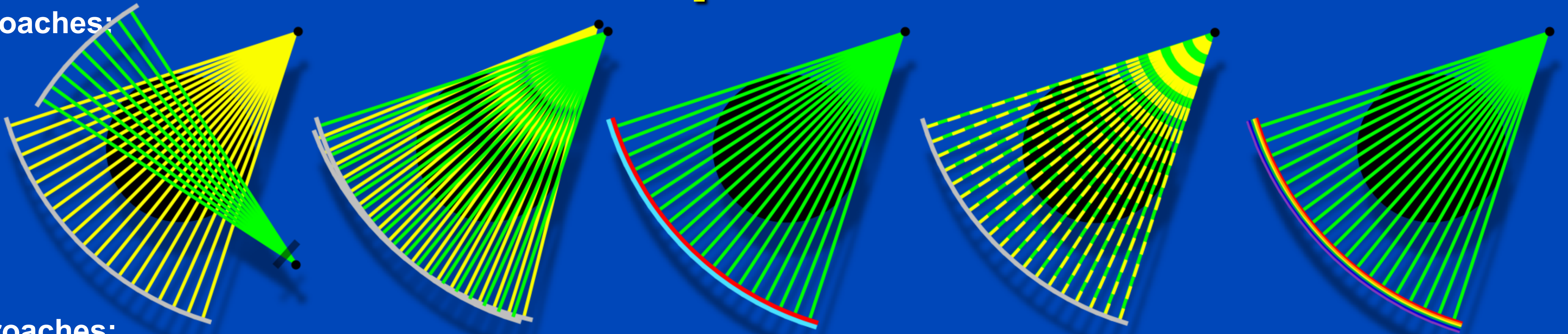

Existing fake spectral CT approaches:

[1] J. Ma, Y. Liao, Y. Wang, S. Li, J. He, D. Zeng, Z. Bian, "Pseudo dual energy CT imaging using deep learning-based framework: basic material estimation", *SPIE Medical Imaging 2018*.

[2] W. Zhao, T. Lv, P. Gao, L. Shen, X. Dai, K. Cheng, M. Jia, Y. Chen, L. Xing, "A deep learning approach for dual-energy CT imaging using a single-energy CT data", *Fully3D 2019.*

[3] D. Lee, H. Kim, B. Choi, H. J. Kim, "Development of a deep neural network for generating synthetic dual-energy chest x-ray images with single x-ray exposure", PMB 64(11), 2019.

[4] L. Yao, S. Li, D. Li, M. Zhu, Q. Gao, S. Zhang, Z. Bian, J. Huang, D. Zeng, J. Ma, "Leveraging deep generative model for direct energy-resolving CT imaging via existing energy-integrating CT images", *SPIE Medical Imaging 2020.*

[5] D. P. Clark, F. R. Schwartz, D. Marin, J. C. Ramirez-Giraldo, C. T. Badea, "Deep learning based spectral extrapolation for dual-source, dual-energy x-ray CT", Med. Phys. 47 (9): 4150–4163, 2020.

[6] C. K. Liu, C. C. Liu, C. H. Yang, H. M. Huang, "Generation of brain dual-energy CT from single-energy CT using deep learning", Journal of Digital Imaging 34(1):149–161, 2021.

[7] T. Lyu, W. Zhao, Y. Zhu, Z. Wu, Y. Zhang, Y. Chen, L. Luo, S. Li, L. Xing, "Estimating dual-energy CT imaging from single-energy CT data with material decomposition convolutional neural network", Medical Image Analysis 70:1–10, 2021.

[8] F. R. Schwartz, D. P. Clark, Y. Ding, J. C. Ramirez-Giraldo, C. T. Badea, D. Marin, "Evaluating renal lesions using deep-learning based extension of dual-energy FoV in dual-source CT—A retrospective pilot study", European Journal of Radiology 139:109734, 2021.

[9] Y. Li, X. Tie, K. Li, J. W. Garrett, G.-H. Chen, "Deep-En-Chroma: mining the spectral fingerprints in single-kV CT acquisitions using energy integration detectors", *SPIE Medical Imaging 2022.*

…

[19] T. Wang, C. Jiang, W. Ding, Q. Chen, D. Shen, Z. Ding, "Deep-learning generated synthetic material decomposition images based on single-energy CT to differentiate intracranial hemorrhage and contrast staining within 24 hours after endovascular thrombectomy", CNS Neurosci. Ther. 31(1), 2025.

J. Maier, J. Erath, S. Sawall, E. Fournié, K. Stierstorfer, and M. Kachelrieß. Raw data consistent deep learning-based field of view extension for dual-source dual-energy CT. Med. Phys. 51(3):1822-1831, March 2024.

[1] J. Ma, Y. Liao, Y. Wang, S. Li, J. He, D. Zeng, Z. Bian, "Pseudo dual energy CT imaging using deep learning-based framework: basic material estimation", *SPIE Medical Imaging 2018.*

[2] W. Zhao, T. Lv, P. Gao, L. Shen, X. Dai, K. Cheng, M. Jia, Y. Chen, L. Xing, "A deep learning approach for dual-energy CT imaging using a single-energy CT data", *Fully3D 2019.*

[3] D. Lee, H. Kim, B. Choi, H. J. Kim, "Development of a deep neural network for generating synthetic dual-energy chest x-ray images with single x-ray exposure", PMB 64(11), 2019.

[4] L. Yao, S. Li, D. Li, M. Zhu, Q. Gao, S. Zhang, Z. Bian, J. Huang, D. Zeng, J. Ma, "Leveraging deep generative model for direct energy-resolving CT imaging via existing energy-integrating CT images", *SPIE Medical Imaging 2020*.

[5] D. P. Clark, F. R. Schwartz, D. Marin, J. C. Ramirez-Giraldo, C. T. Badea, "Deep learning based spectral extrapolation for dual-source, dual-energy x-ray CT", Med. Phys. 47 (9): 4150–4163, 2020.

[6] C. K. Liu, C. C. Liu, C. H. Yang, H. M. Huang, "Generation of brain dual-energy CT from single-energy CT using deep learning", Journal of Digital Imaging 34(1):149–161, 2021.

[7] T. Lyu, W. Zhao, Y. Zhu, Z. Wu, Y. Zhang, Y. Chen, L. Luo, S. Li, L. Xing, "Estimating dual-energy CT imaging from single-energy CT data with material decomposition convolutional neural network", Medical Image Analysis 70:1–10, 2021.

[8] F. R. Schwartz, D. P. Clark, Y. Ding, J. C. Ramirez-Giraldo, C. T. Badea, D. Marin, "Evaluating renal lesions using deep-learning based extension of dual-energy FoV in dual-source CT—A retrospective pilot study", European Journal of Radiology 139:109734, 2021.

[9] Y. Li, X. Tie, K. Li, J. W. Garrett, G.-H. Chen, "Deep-En-Chroma: mining the spectral fingerprints in single-kV CT acquisitions using energy integration detectors", *SPIE Medical Imaging 2022.*

[10] S. Charyyev, T. Wang, Y. Lei, B. Ghavidel, J. J. Beitler, M. McDonald, W. J. Curran, T. Liu, J. Zhou, X. Yang, "Learning-based synthetic dual energy CT imaging from single energy CT for stopping power ratio calculation in proton radiation therapy", Brit. J. Radiol. 95(1129), 2022.

[11] J. Jeong, A. Wentland, D. Mastrodicasa, G. Fananapazir, A. Wang, I. Banerjee, B. N. Patel, "Synthetic dual-energy CT reconstruction from single-energy CT Using artificial intelligence", Abdom. Radiol. 48 (11): 3537–3549, 2023.

[12] Y. Li, X. Tie, K. Li, R. Zhang, Z. Qi, A. Budde, T. M. Grist, G.-H. Chen, "A quality-checked and physics-constrained deep learning method to estimate material basis images from single-kV contrast-enhanced chest CT scans", Med. Phys. 50(6):3368-3388, June 2023.

[13] S. Kim, J. Lee, J. Kim, B. Kim, C. H. Choi, S. Jung, "Conversion of single-energy CT to parametric maps of dual-energy CT using convolutional neural network", ", Brit. J. Radiol. 97 (1158): 1180–1190, 2024.

[14] Y. Koike, S. Ohira, S. Kihara, Y. Anetai, H. Takegawa, S. Nakamura, M. Miyazaki, K. Konishi, N. Tanigawa, "Synthetic low-energy monochromatic image generation in single-energy computed tomography system using a transformer-based deep learning model", J. Imaging Inform. Med. (5): 2688–2697, 2024.

[15] M. Lee, H. Lee, D. Lee, H. Cho, J. Choi, B. K. Cha, K. Kim, "Framework for dual-energy-like chest radiography image synthesis from single-energy computed tomography based on cycle-consistent generative adversarial network", Med. Phys. 51 (2): 1509–1530, 2024.

[16] Y. Gao, H. Xie, C. W. Chang, J. Peng, S. Pan, R. L. J. Qiu, T. Wang, B. Ghavidel, J. Roper, J. Zhou, X. Yang, "CT-based synthetic iodine map generation using conditional denoising diffusion probabilistic model", Med. Phys. 51(9): 6246–6258, 2024.

[17] Y. Gao, H. Xie, C.-W. Chang, J. Peng, R. L. J. Qiu, T. Wang, J. Roper, B. Ghavidel, J. Zhou, X. Yang, "Iodine map synthesis from non-contrast CT using diffusion model", SPIE Medical Imaging 2024.

[18] Y. Gao, R. L. J. Qiu, H. Xie, C. W. Chang, T. Wang, B. Ghavidel, J. Roper, J. Zhou, X. Yang, "CT-based synthetic contrast-enhanced dual-energy CT generation using conditional denoising diffusion probabilistic model", Phys. Med. Biol. 69(16): 165015, 2024.

[19] T. Wang, C. Jiang, W. Ding, Q. Chen, D. Shen, Z. Ding, "Deep-learning generated synthetic material decomposition images based on single-energy CT to differentiate intracranial hemorrhage and contrast staining within 24 hours after endovascular thrombectomy", CNS Neurosci. Ther. 31(1), 2025.

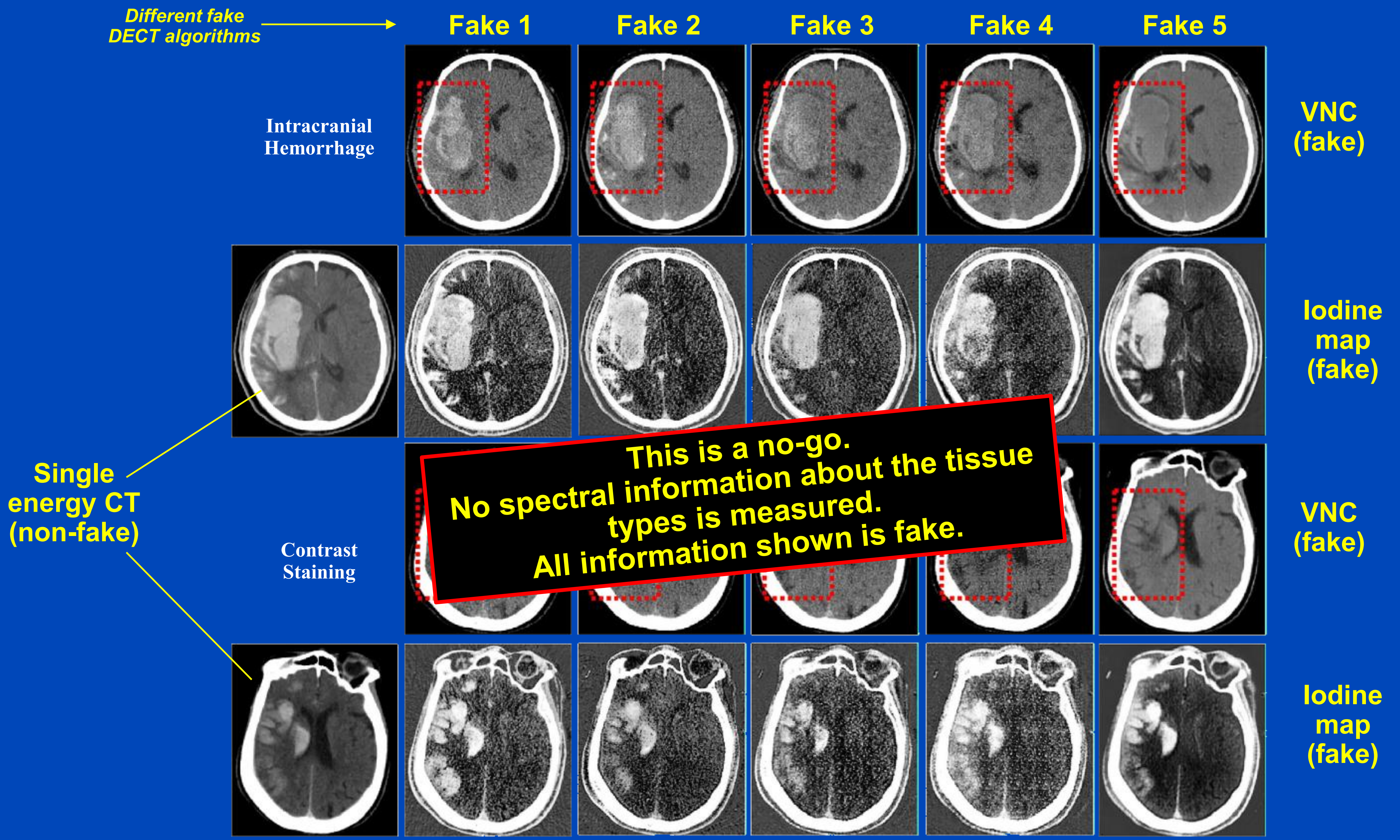

Figure taken from T. Wang, C. Jiang, W. Ding, Q. Chen, D. Shen, Z. Ding, "Deep-learning generated synthetic material decomposition images based on single-energy CT to differentiate intracranial hemorrhage and contrast staining within 24 hours after endovascular thrombectomy", CNS Neurosci. Ther. 31(1), 2025.

dkfz.

Deep Cosmetic Motion Artifact Reduction

- Image-based correction
  = cosmetic correction
  = similar to pic beauty and others
- May not be the most confident way to go

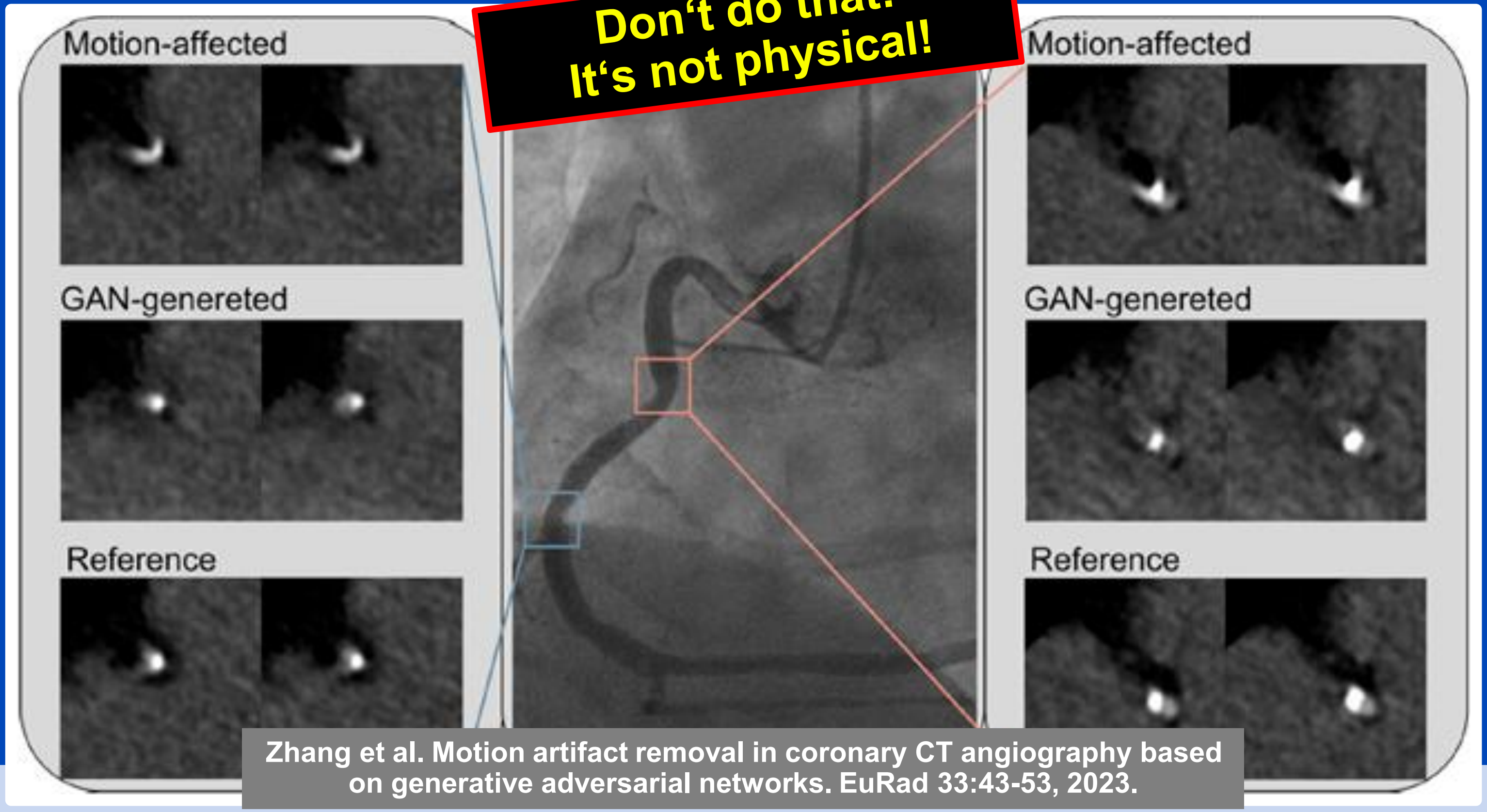

Zhang et al. Motion artifact removal in coronary CT angiography based on generative adversarial networks. EuRad 33:43-53, 2023.

Motion Compensation = Let the Voxels Move!

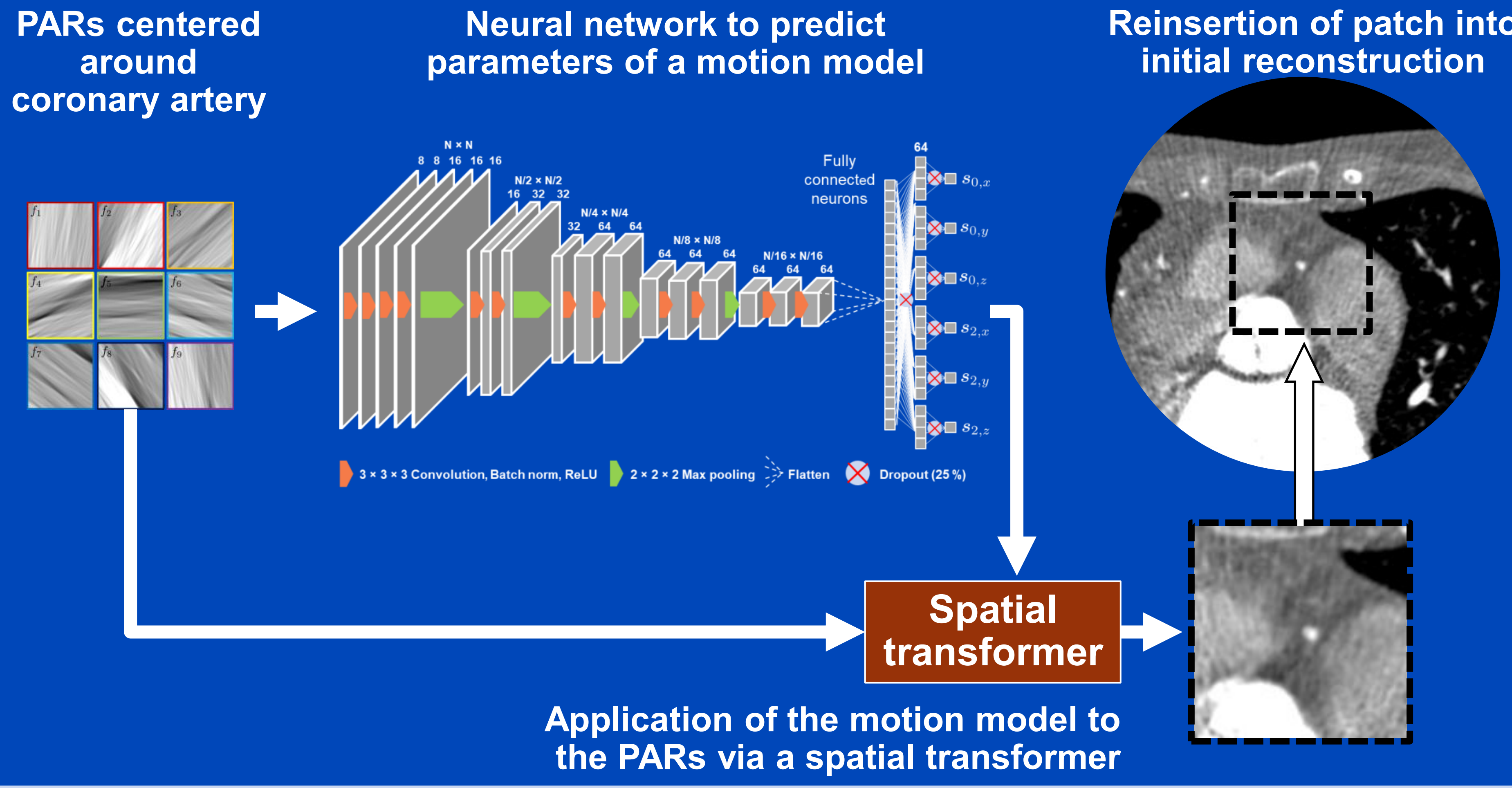

J. Maier, S. Lebedev, J. Erath, E. Eulig, S. Sawall, E. Fournié, K. Stierstorfer, M. Lell, and M. Kachelrieß. Deep learning-based coronary artery motion estimation and compensation for short-scan cardiac CT. Med. Phys. 48(7):3559-3571, July 2021.

Results

Measurements at a Siemens Somatom AS, patient 1

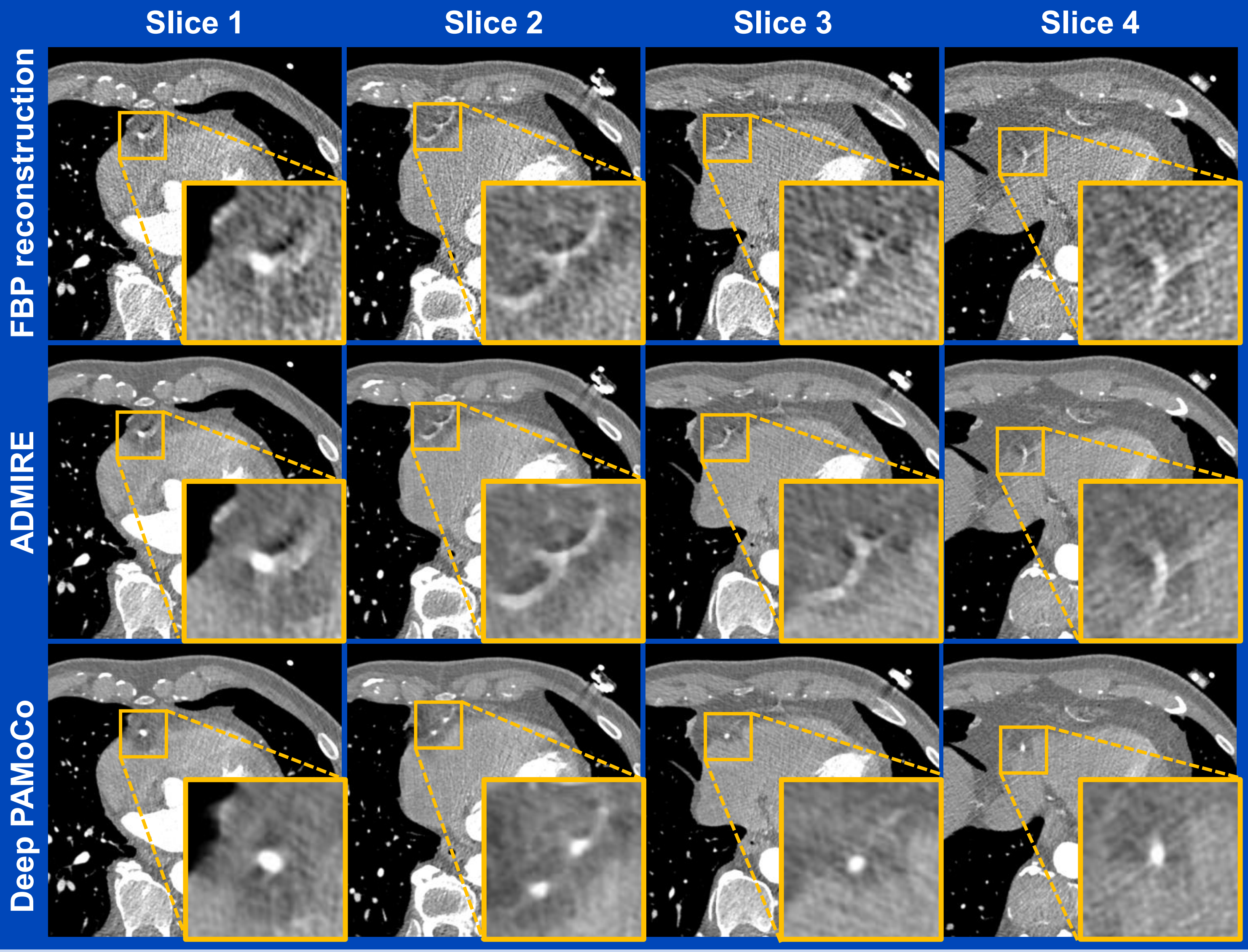

C = 0 HU, *W* = 1200 HU

J. Maier, S. Lebedev, J. Erath, E. Eulig, S. Sawall, E. Fournié, K. Stierstorfer, M. Lell, and M. Kachelrieß. Deep learning-based coronary artery motion estimation and compensation for short-scan cardiac CT. Med. Phys. 48(7):3559-3571, July 2021.

Noise Removal: Canon's AiCE

- Advanced intelligent Clear-IQ Engine (AiCE)
- Trained to restore low-dose CT data to match the properties of FIRST, the model-based IR of Canon.
- FIRST is applied to high-dose CT images to obtain a high fidelity training target

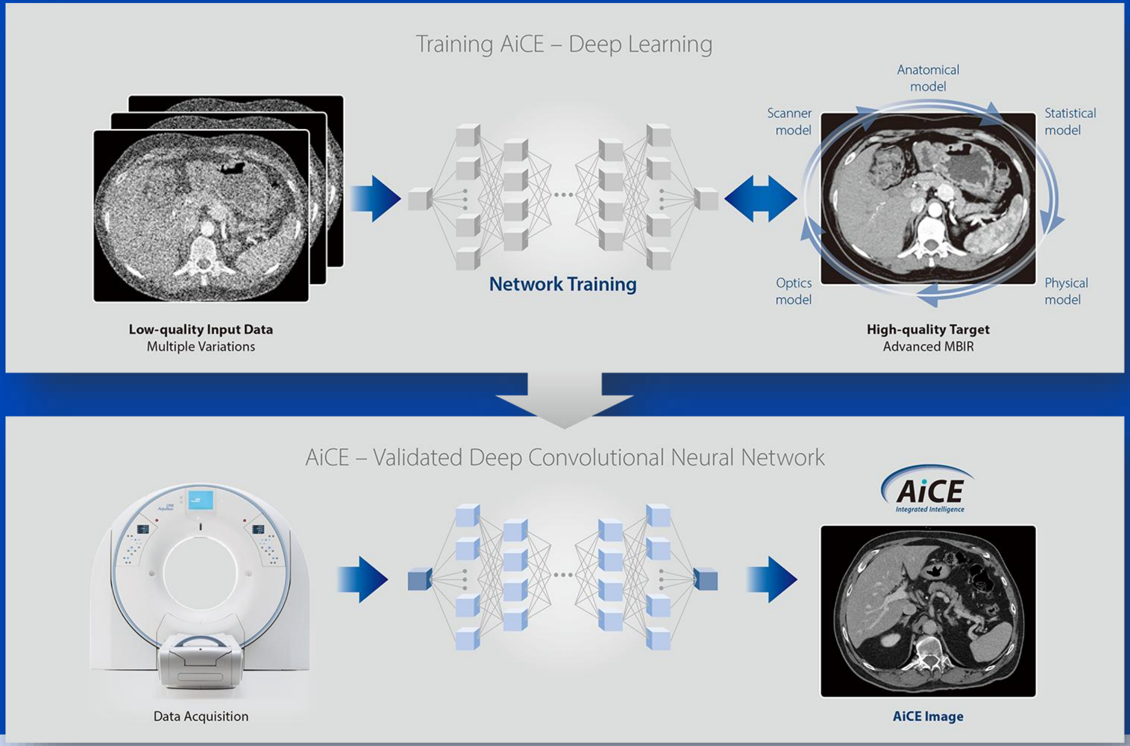

K. Boedeker. AiCE Deep Learning Reconstruction: Bringing the Power of Ultra High Resolution CT to Routine Imaging. Whitepaper, Canon, 2019.

U = 100 kV
CTDI = 0.6 mGy
DLP = 24.7 mGy·cm
D_{eff} = 0.35 mSv

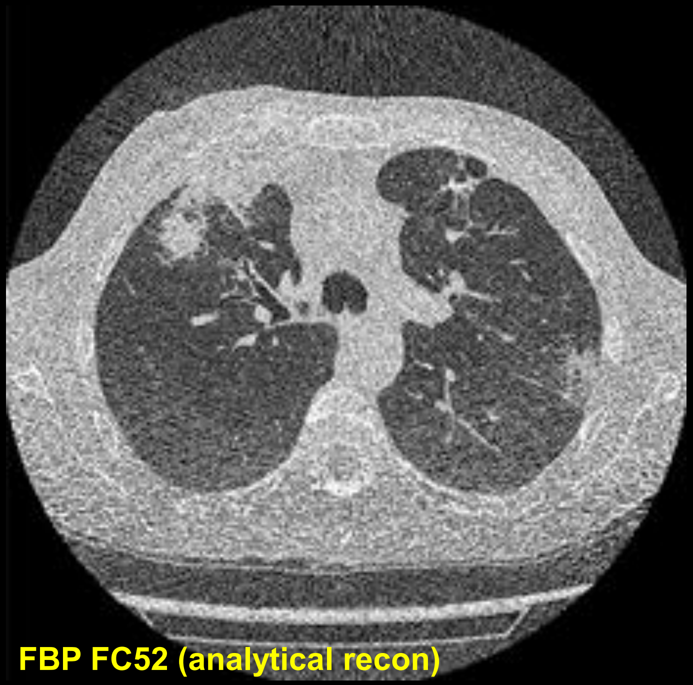

FBP FC52 (analytical recon)

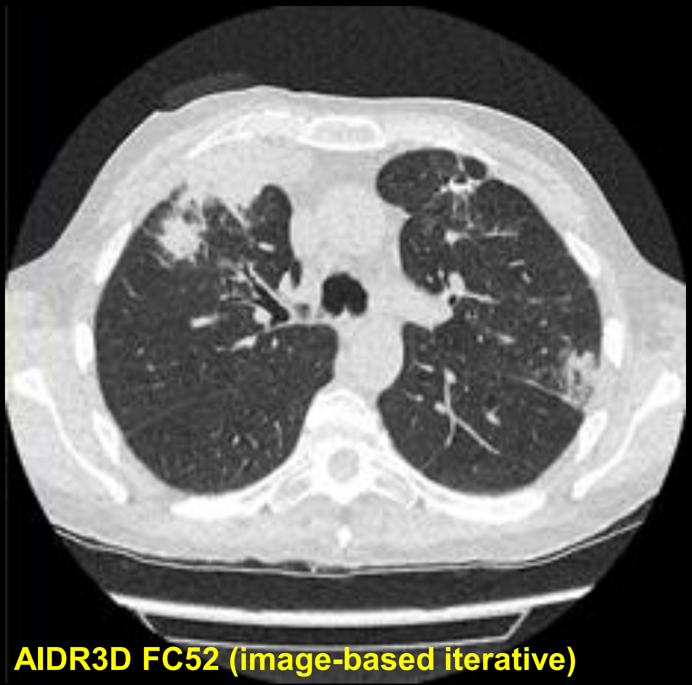

AIDR3D FC52 (image-based iterative)

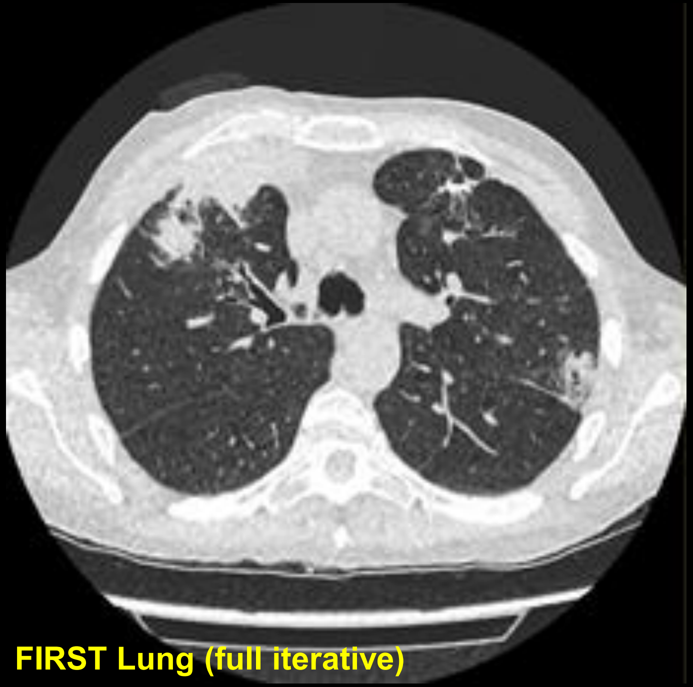

FIRST Lung (full iterative)

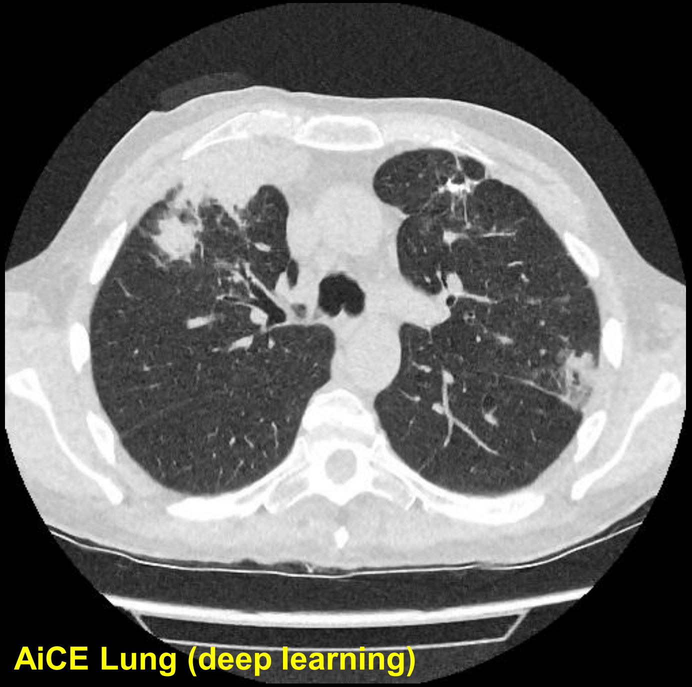

AiCE Lung (deep learning)

Courtesy of
Radboudumc,
the Netherlands

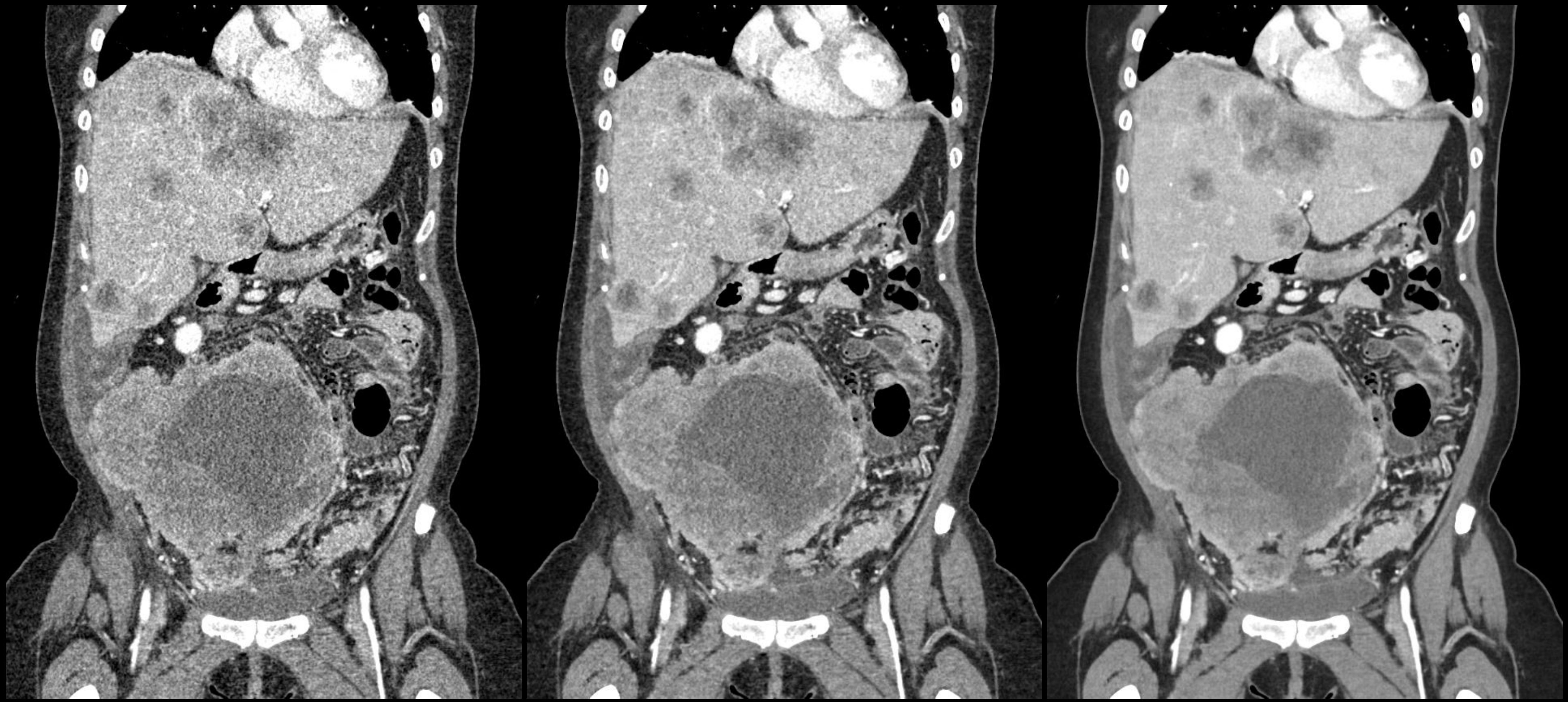

FBP

ASIR V 50%

True Fidelity

Courtesy of GE Healthcare

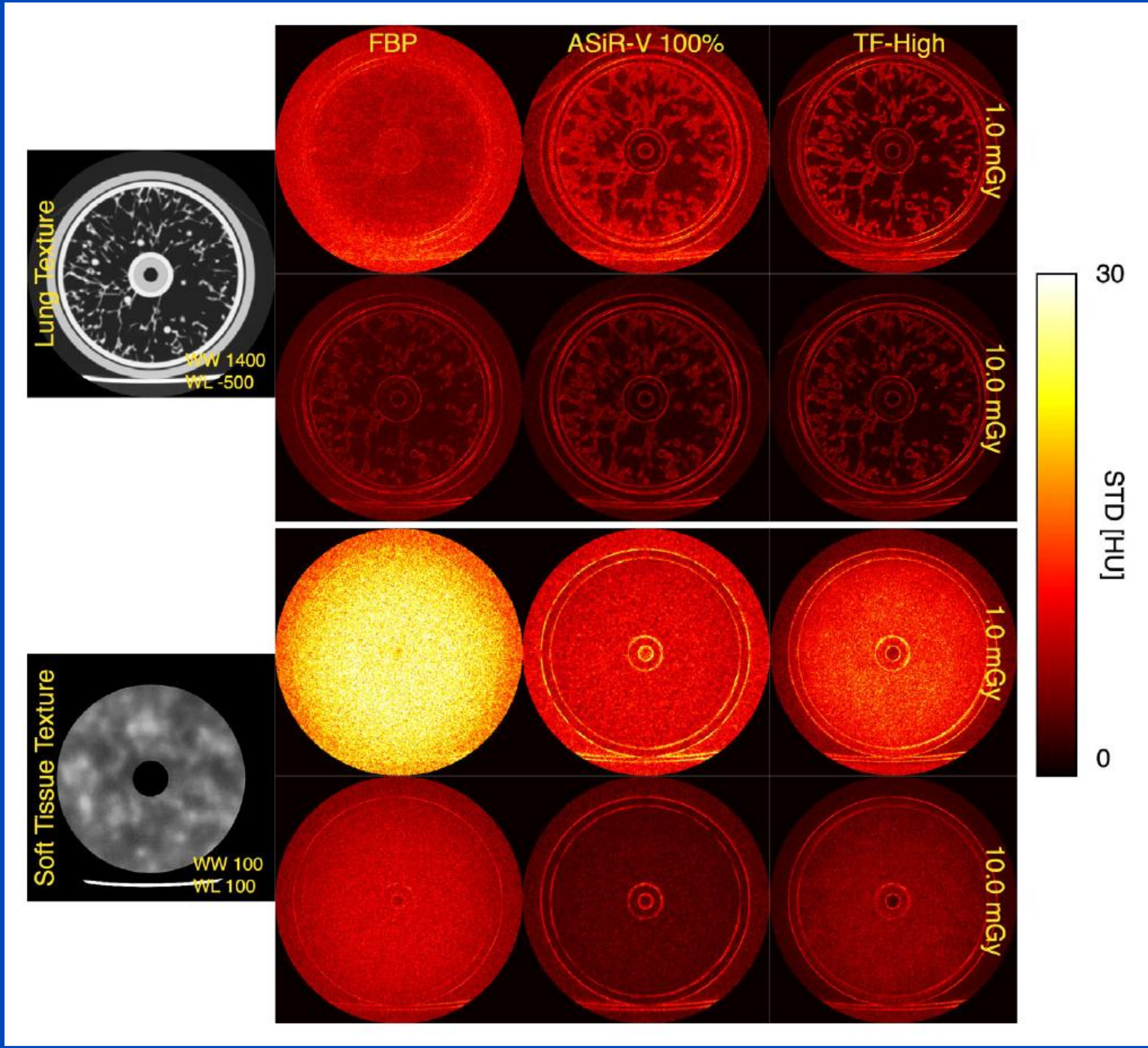

Solomon et al. Noise and spatial resolution properties of a commercially available deep learning-based CT reconstruction algorithm.
Med. Phys. 47(9):3961-3971, Sept. 2020

Noise Removal: Philips' Precise Image

- Noise-injected data serve as low dose examples while their original reconstructions are the labels. A CNN learns how to denoise the low dose images.

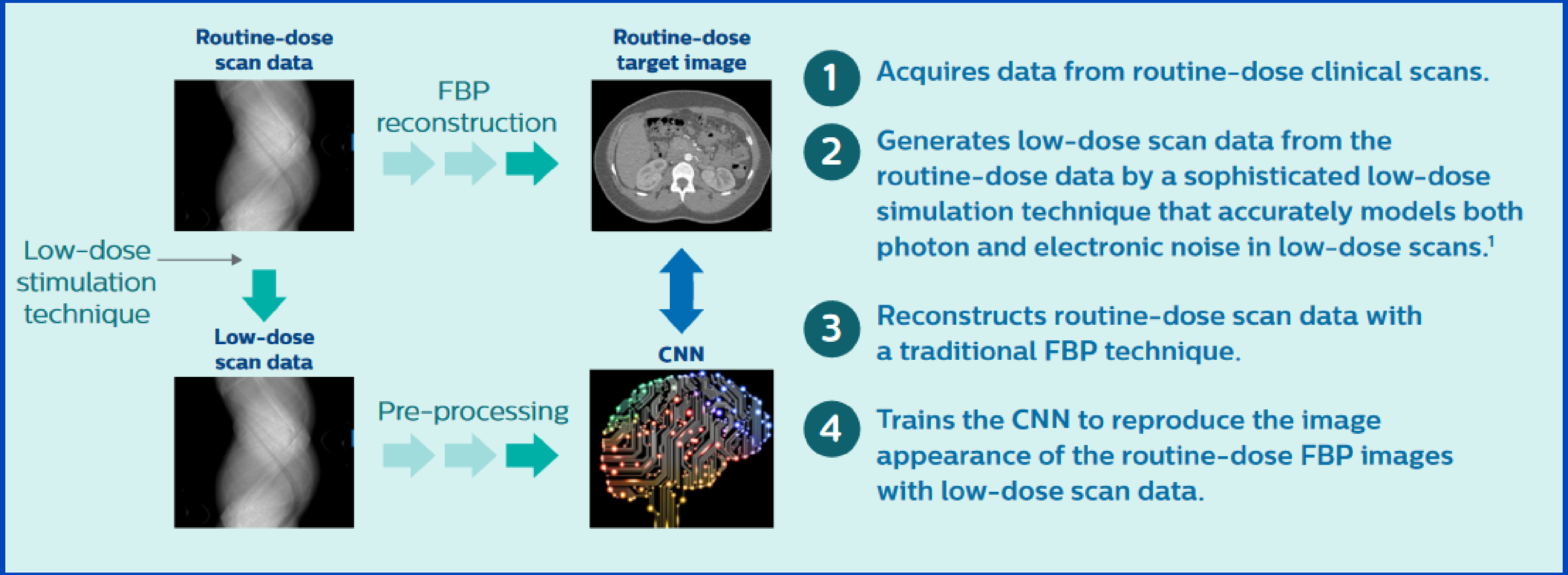

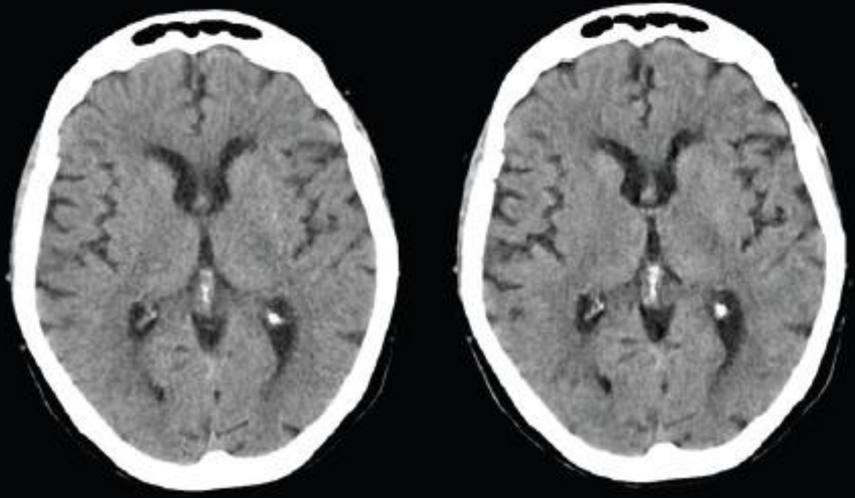

iDose⁴ 1.4 mSv Precise Image 0.7 mSv

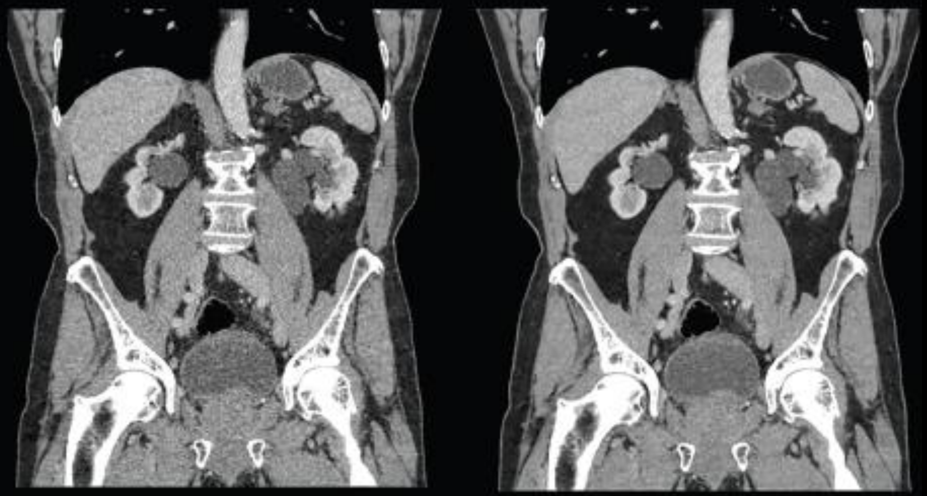

iDose⁴ 5.1 mSv Precise Image 2.6 mSv

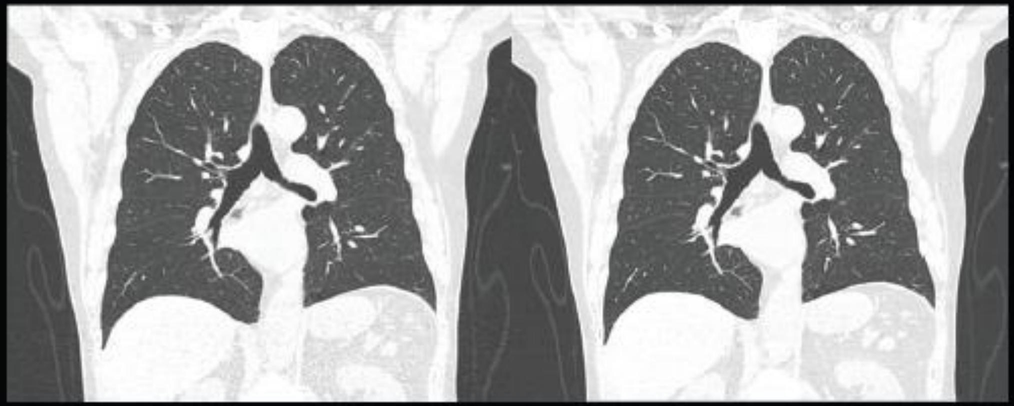

iDose⁴ 1.5 mSv Precise Image 0.75 mSv

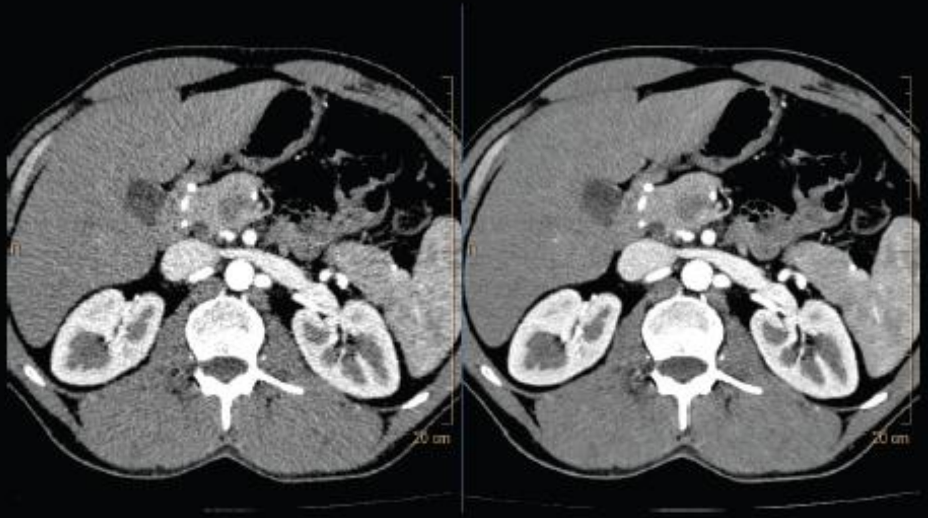

iDose⁴ 5.4 mSv Precise Image 2.6 mSv

Taken from https://www.philips.com/c-dam/b2bhc/master/resource-catalog/landing/precise-suite/incisive_precise_image.pdf

Received: 31 January 2025 | Revised: 22 August 2025 | Accepted: 26 August 2025
DOI: 10.1002/mp.18121

RESEARCH ARTICLE

MEDICAL PHYSICS

Noise-augmented deep denoising: A method to boost CT image denoising networks

Gernot Kristof[1,2] | Elias Eulig[1,2] | Marc Kachelrieß[1,3]

[1]Division of X–Ray Imaging and Computed Tomography, German Cancer Research Center (DKFZ), Heidelberg, Germany

[2]Department of Physics and Astronomy, Heidelberg University, Heidelberg, Germany

[3]Medical Faculty, Heidelberg University, Heidelberg, Germany

Abstract

Background: Denoising low dose computed tomography (CT) images can have great advantages for the aim of minimizing the radiation risk of the patients, as it can help lower the effective dose to the patient while providing constant image quality. In recent years, deep denoising methods became a popular way to accomplish this task. Conventional deep denoising algorithms, however, cannot handle the correlation between neighboring pixels or voxels very well, because

NADD = 1 measurement
+ 10 simulated noise realizations
+ a denoising network

Images and Noise Only Images

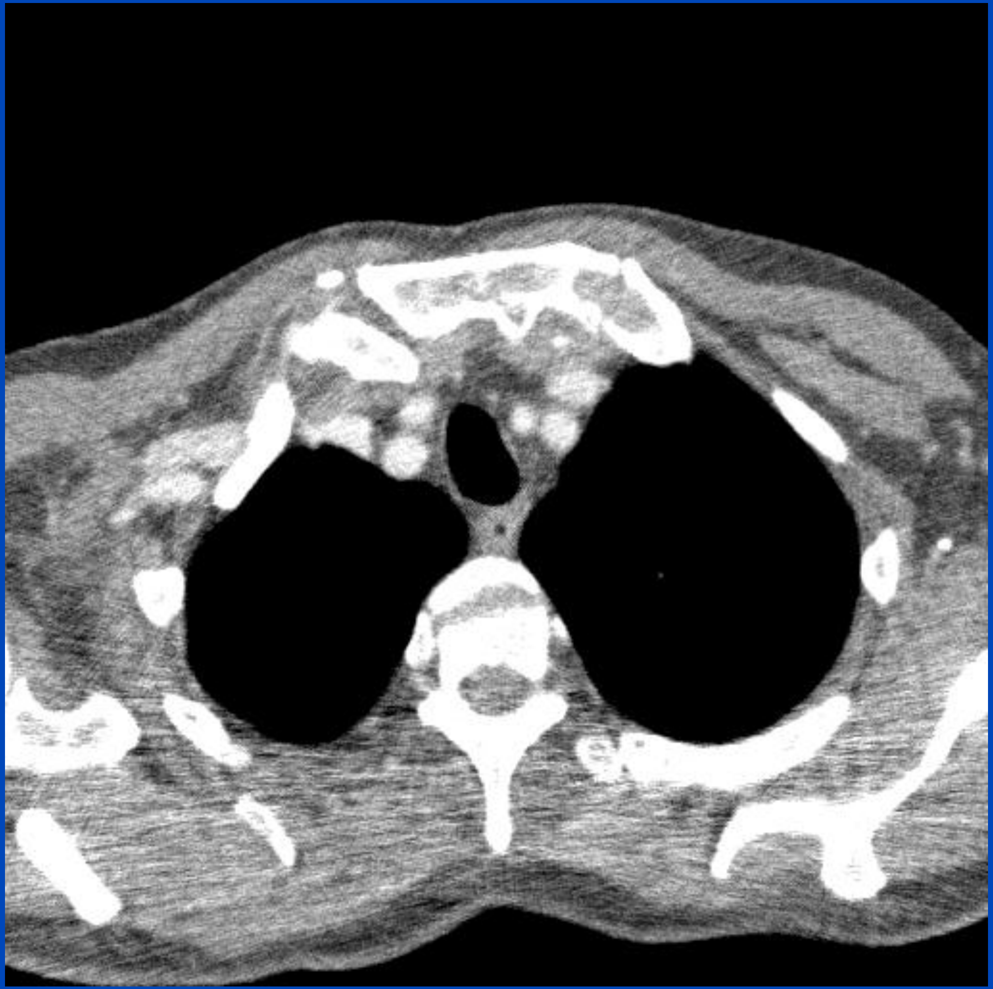

C = 0 HU, W = 600 HU

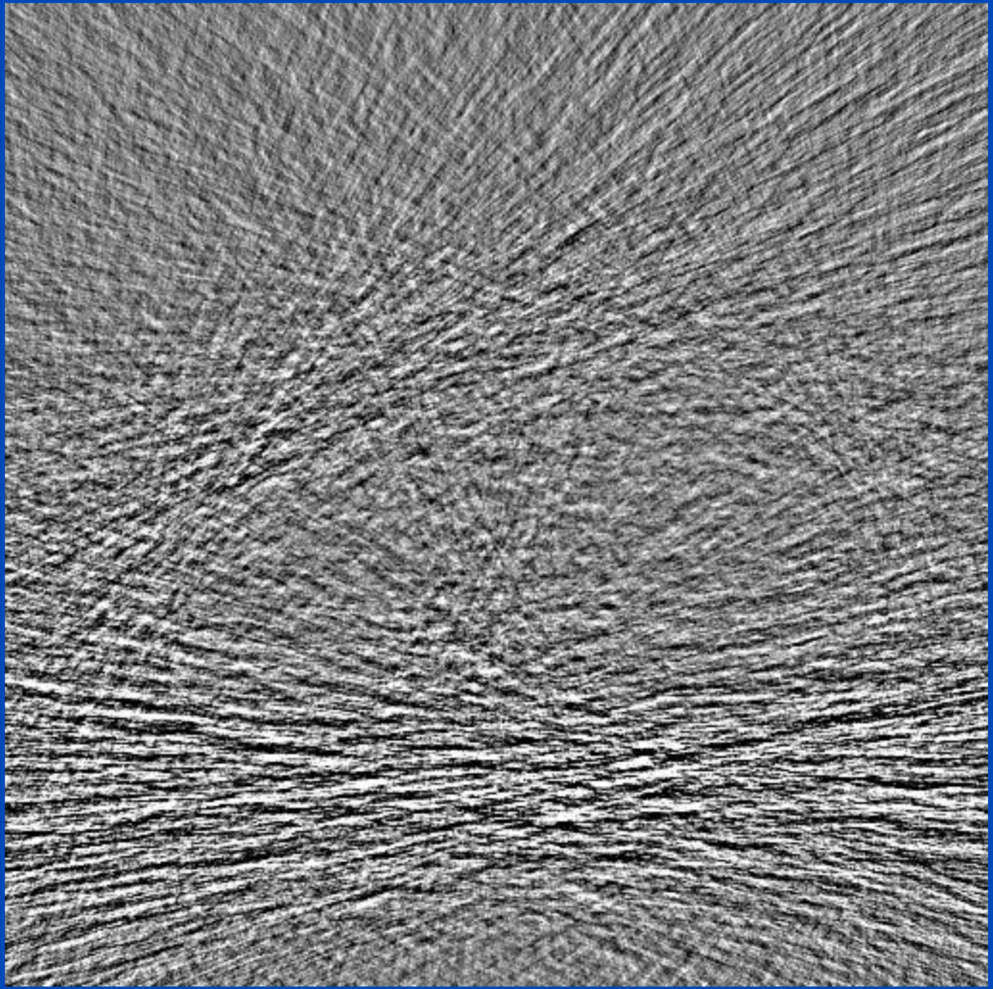

C = 0 HU, W = 150 HU

Images and Noise Only Images

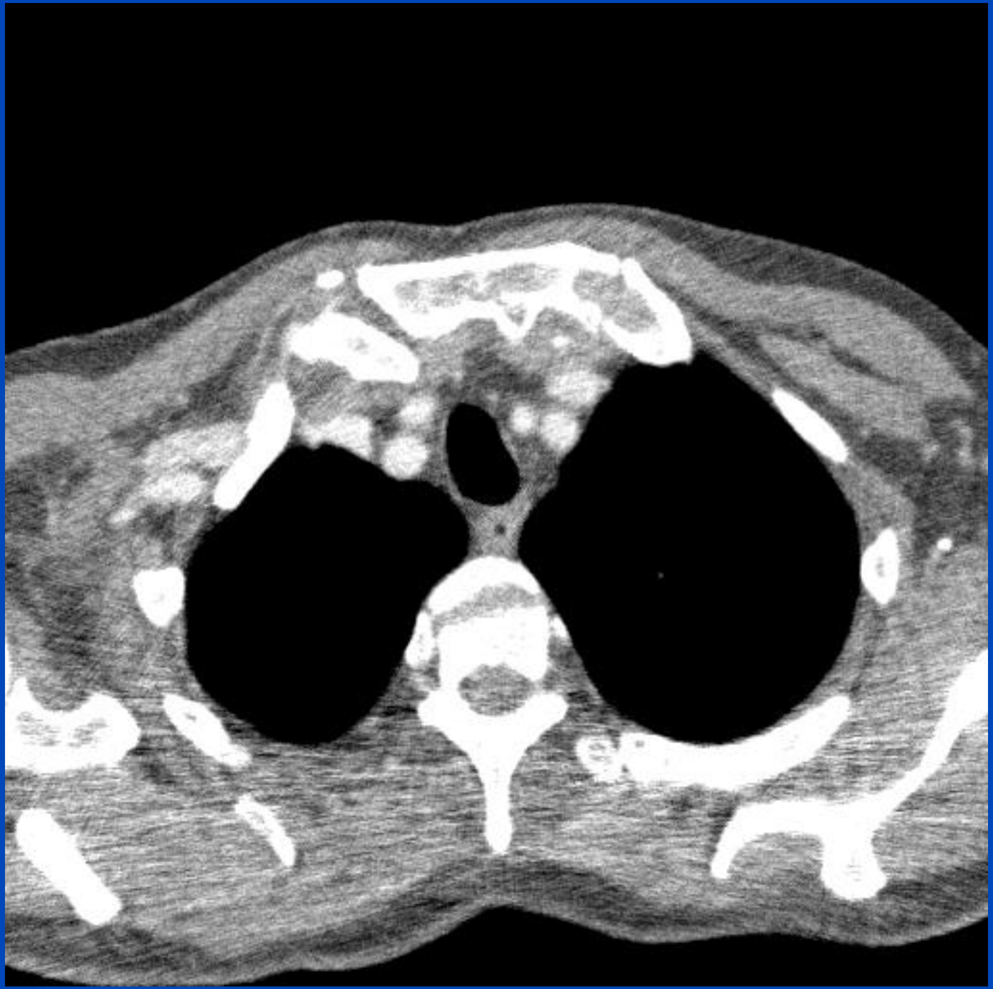

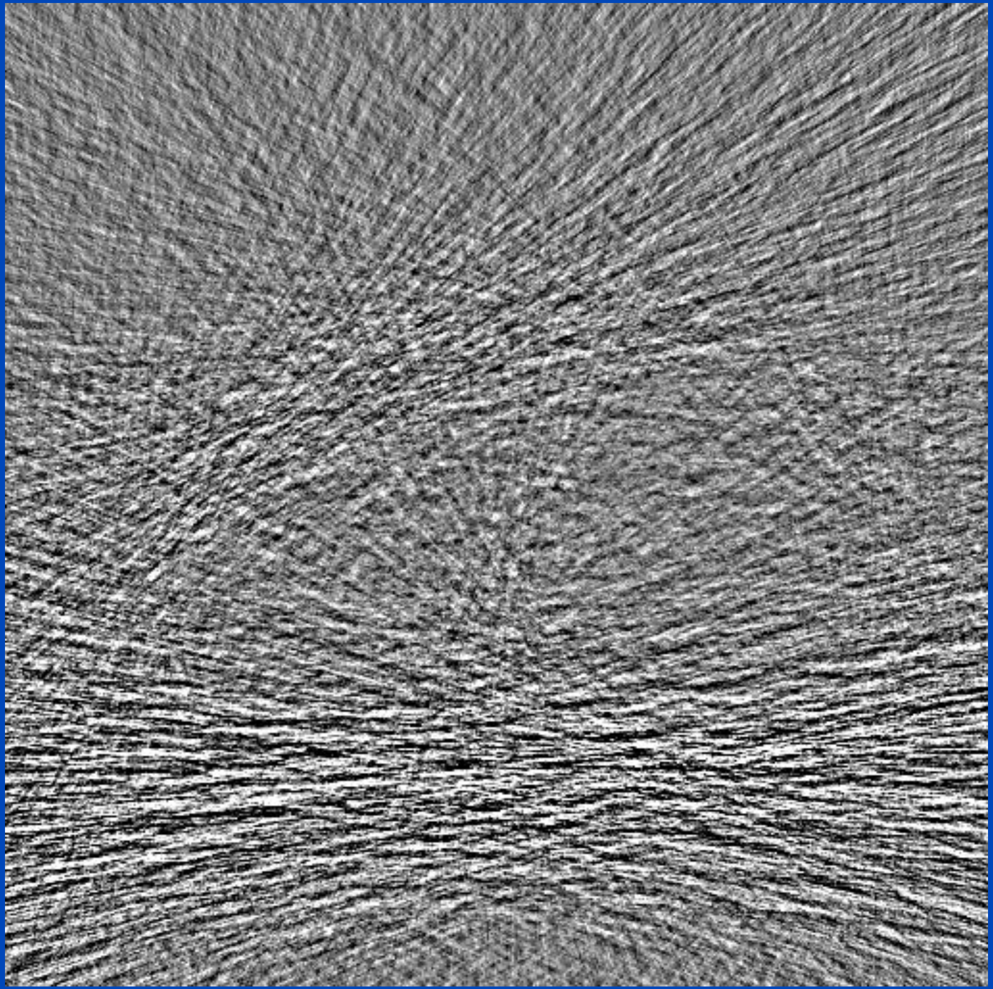

C = 0 HU, *W* = 600 HU

C = 0 HU, *W* = 150 HU

Images and Noise Only Images

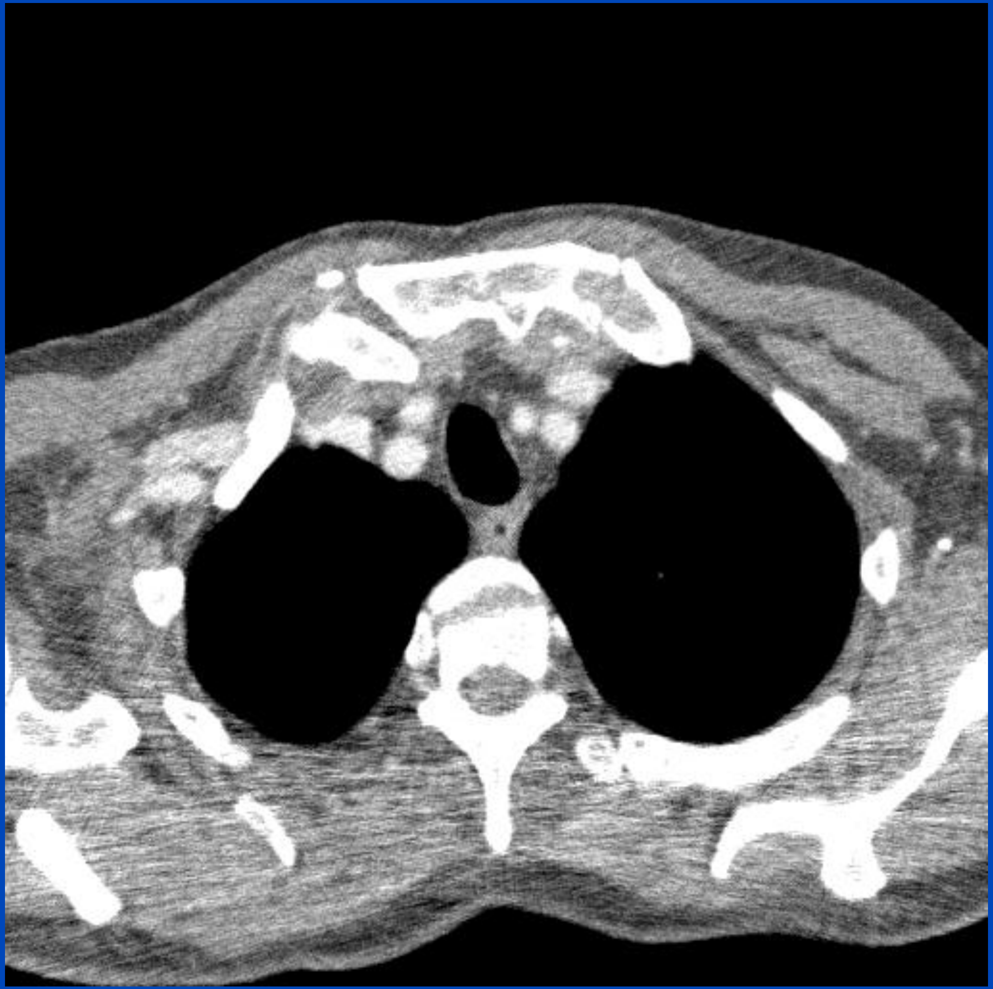

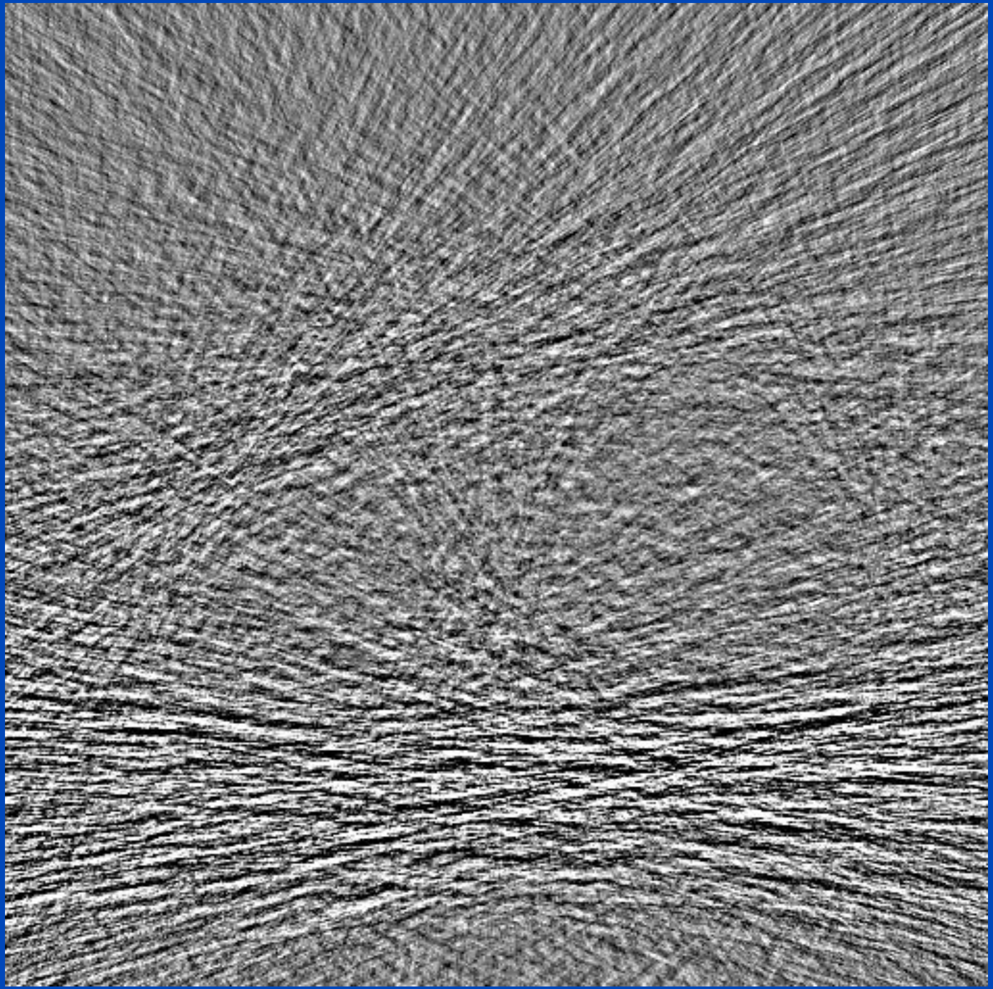

C = 0 HU, *W* = 600 HU

C = 0 HU, *W* = 150 HU

Low Dose, Std Dose and all 10 Noise Only Realizations

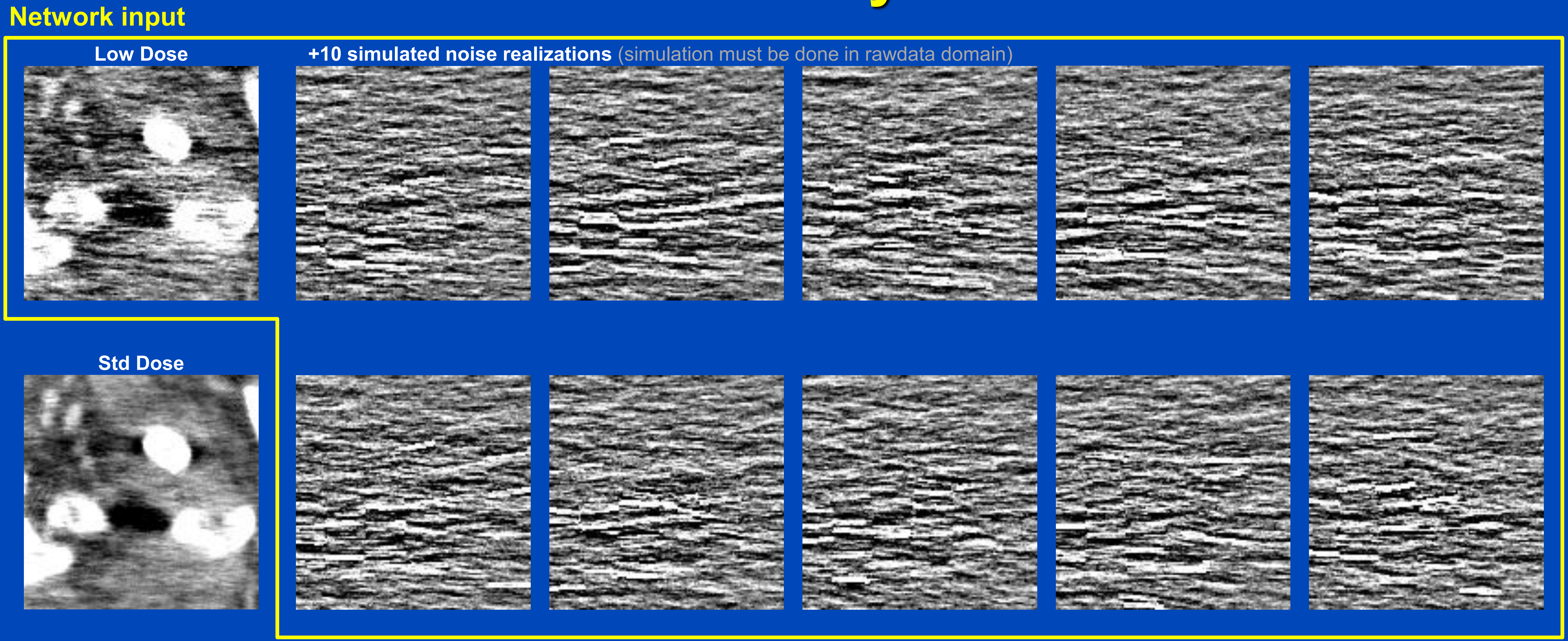

CT Images: C = 0 HU, W = 600 HU. Noise only images: C = 0 HU, W = 550 HU.

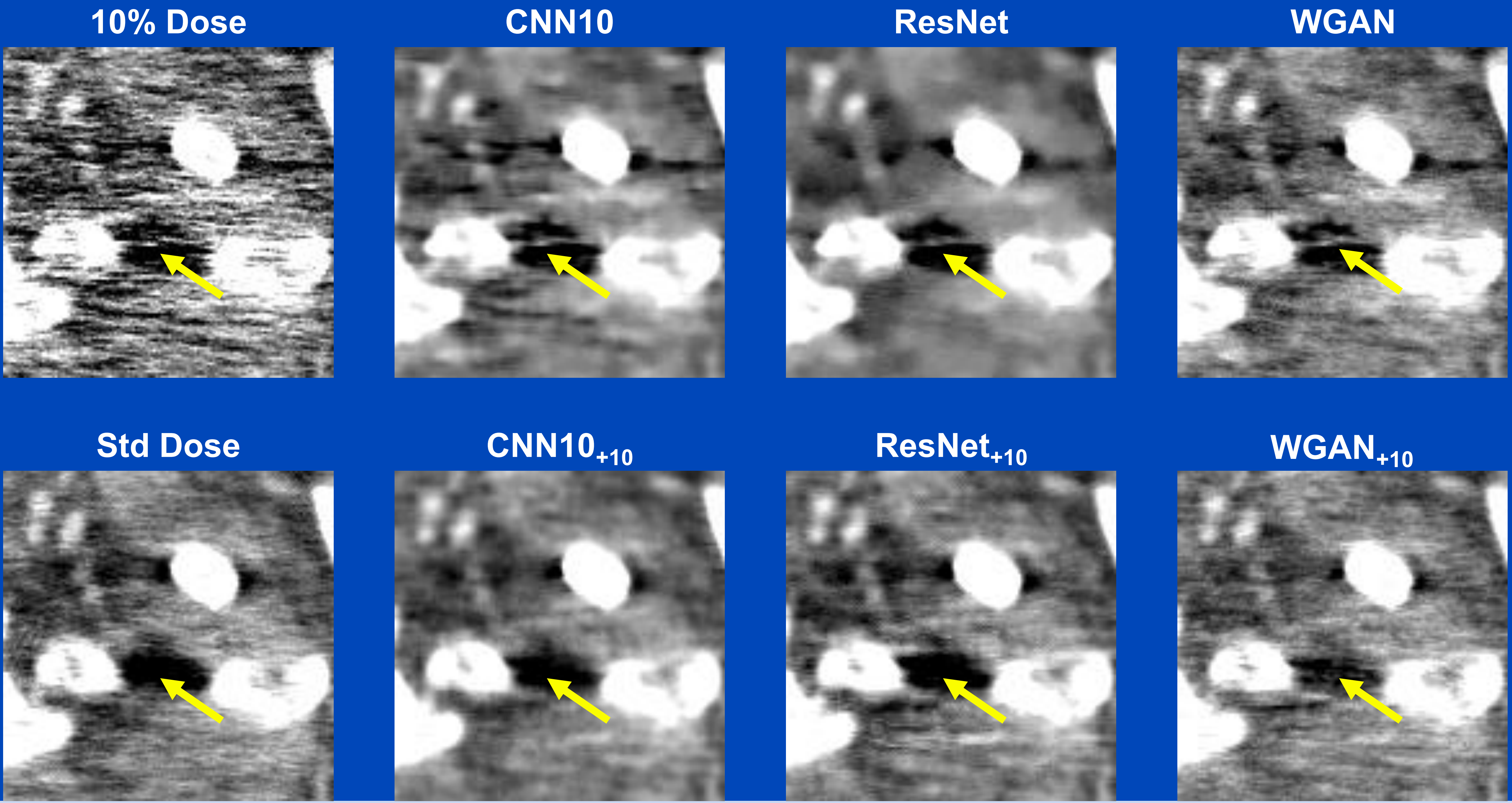

C = 0 HU, W = 600 HU

Results

Std Dose | **10% Dose** | **WGAN**

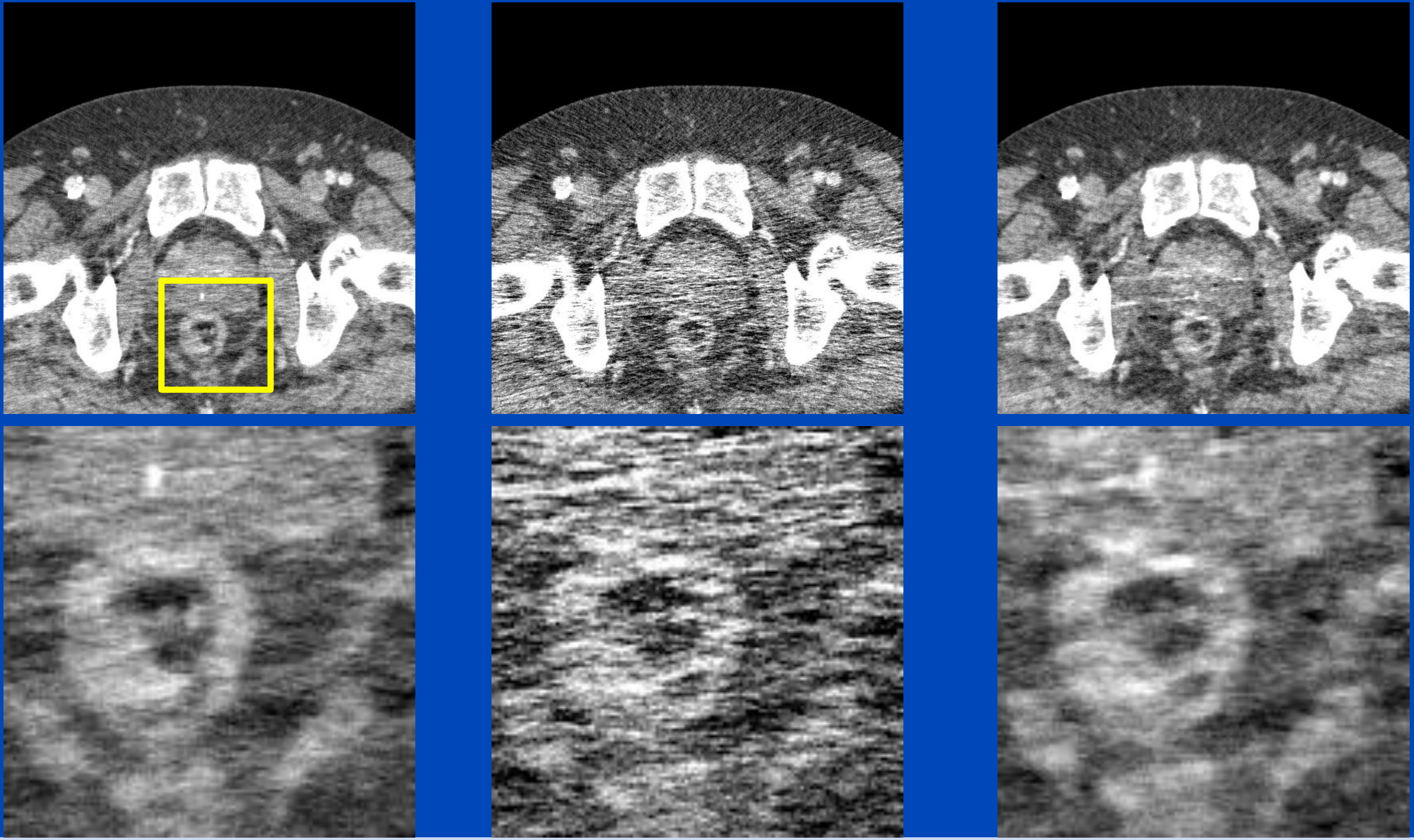

C = 0 HU, *W* = 500 HU

Results

NADD with 10 noise images

Std Dose	10% Dose	WGAN_{+10}

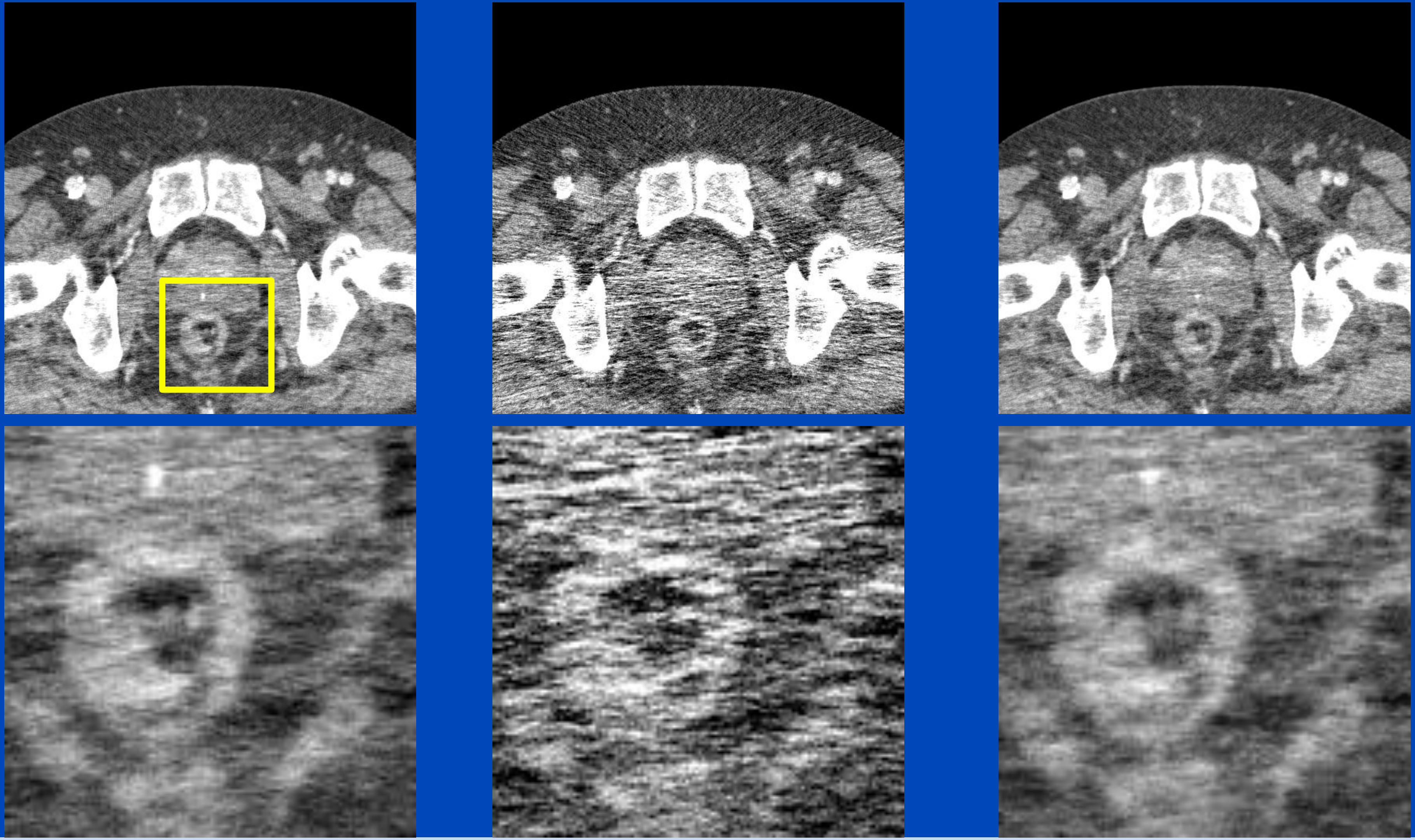

C = 0 HU, W = 500 HU

NADD Results

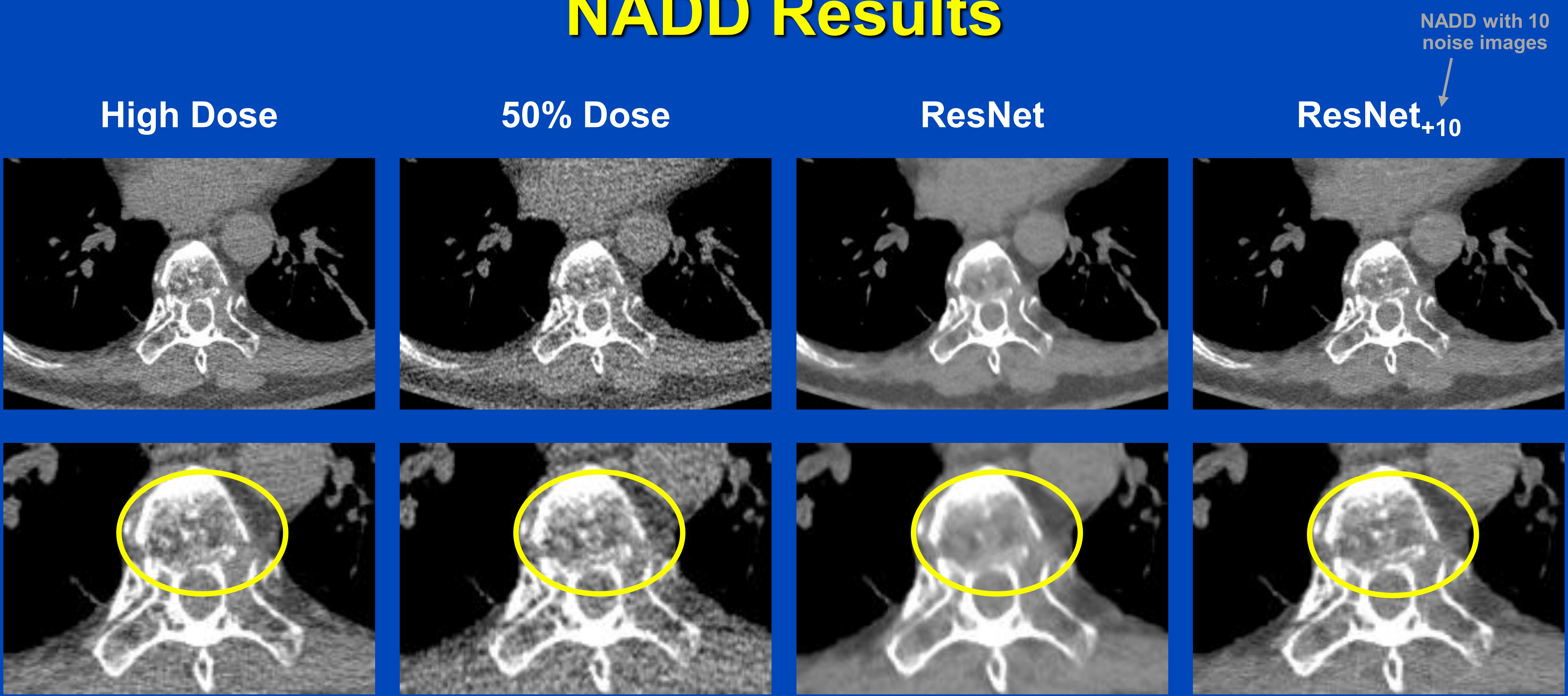

All images reconstructed with ReconCT using the B37f kernel. *C* = 30 HU, *W* = 660 HU

NADD Results

NADD with 10 noise images

High Dose | 50% Dose | ResNet | ResNet$_{+10}$

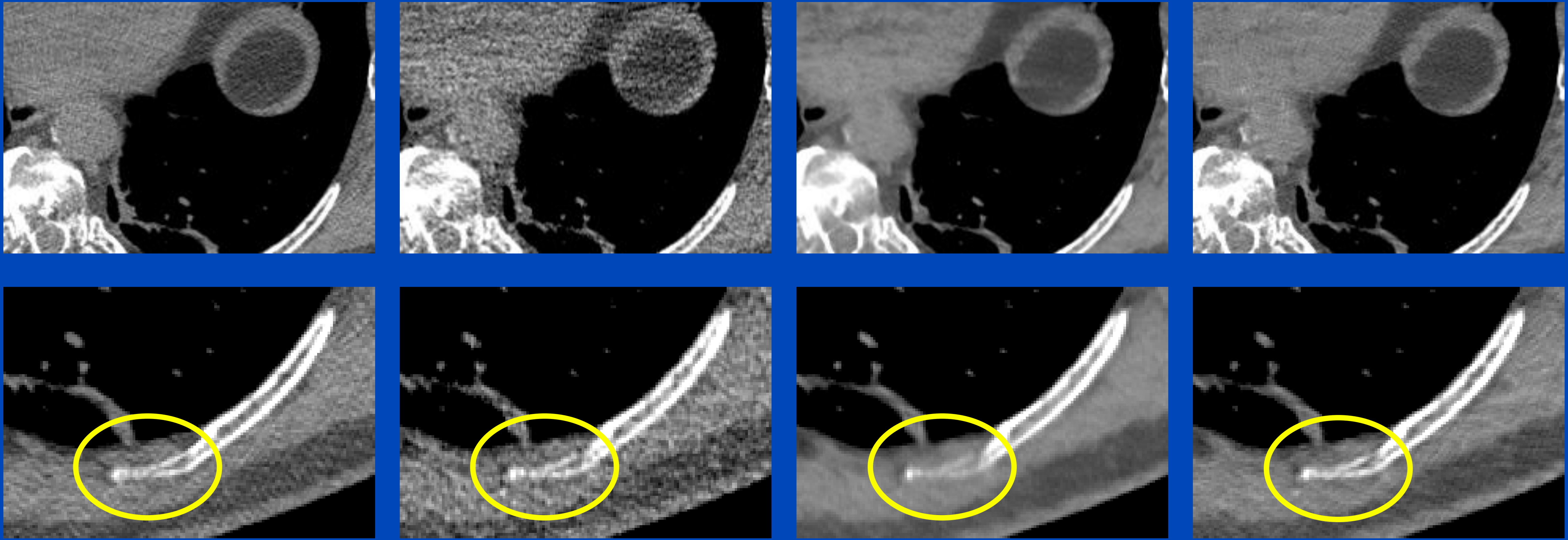

All images reconstructed with ReconCT using the B37f kernel. C = 30 HU, W = 660 HU

Minimize pitfall: Let small structures be just as important as large structures

A NEW METRIC FOR SUBTLE DETAILS

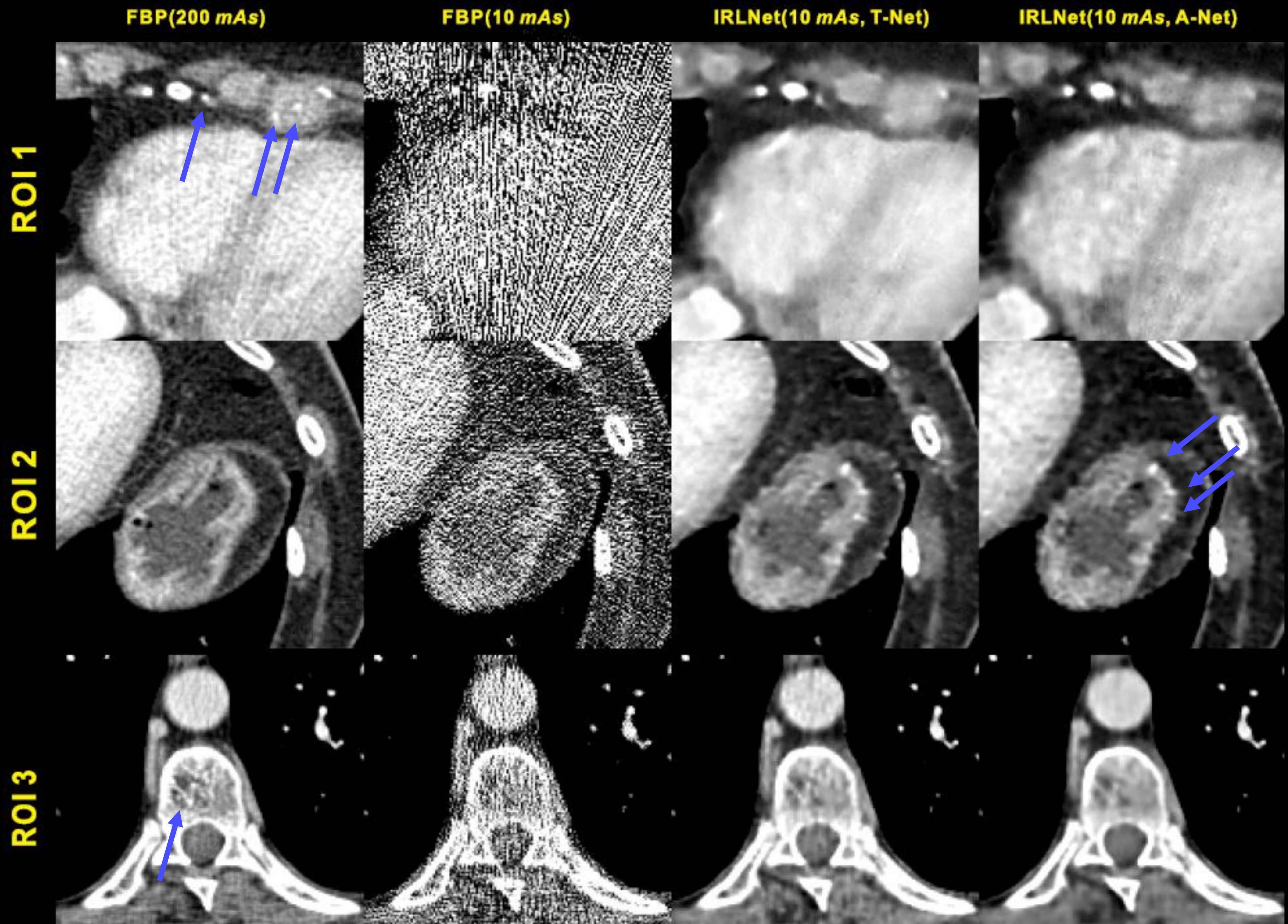

Y. Wang et al. Iterative quality enhancement via residual-artifact learning networks for low-dose CT. Phys. Med. Biol. 63:215004, 2018.

Attention: Each Pixel May be Significant!

- MAE, PSNR, RMSE and SSIM* are often used to quantify image quality, e.g. in loss functions or to rank algorithms.
- Alteration of a few pixels may mislead diagnosis.

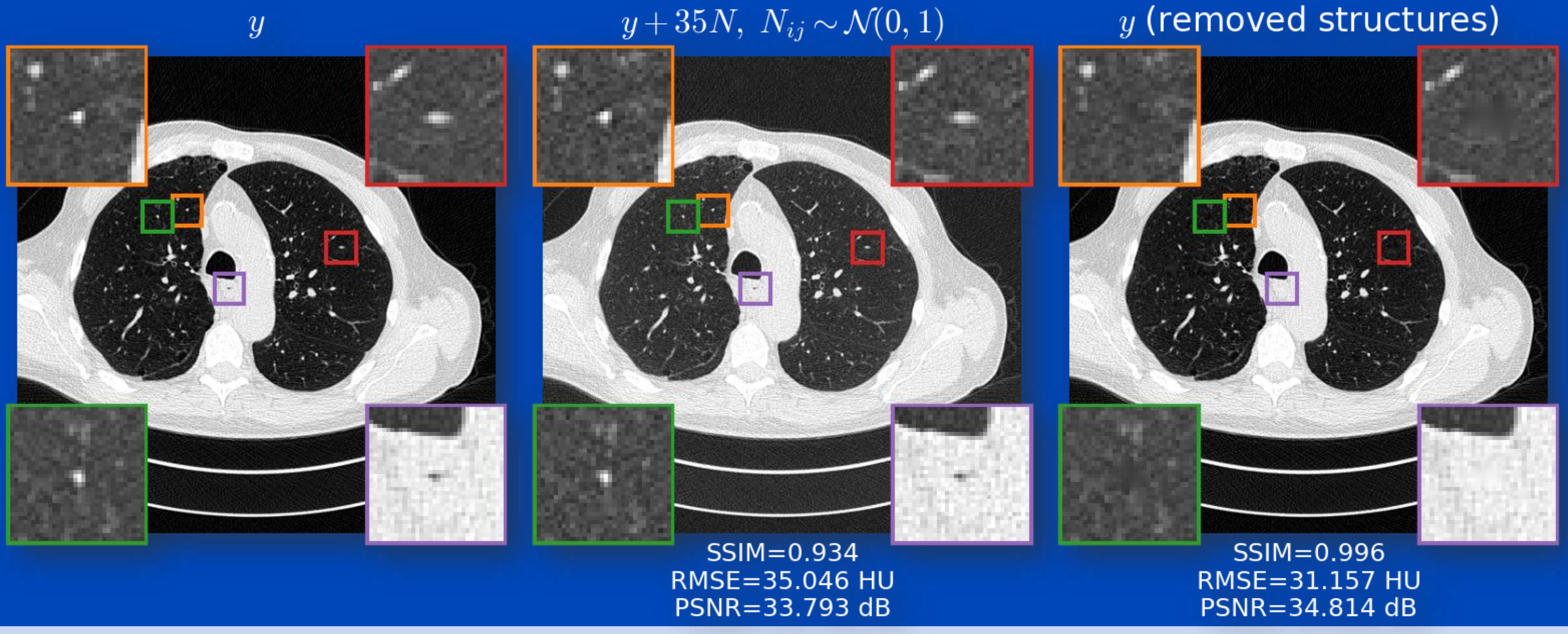

*SSIM also accounts in parts for the human visual system by using luminance, contrast and structure to estimate perceptual quality.

dkfz.

Segment Anything Model (SAM)[1]

- SAM can automatically segment all structures in an image by predicting masks for all points on a grid.
- Many works proposed tuned versions of SAM for medical image segmentation[2]
- To make our metric work, we need to apply SAM
  - to the ground truth image
  - or to the denoised image
  - or to the noisy image.
- In the following, SAM is applied to the GT image.

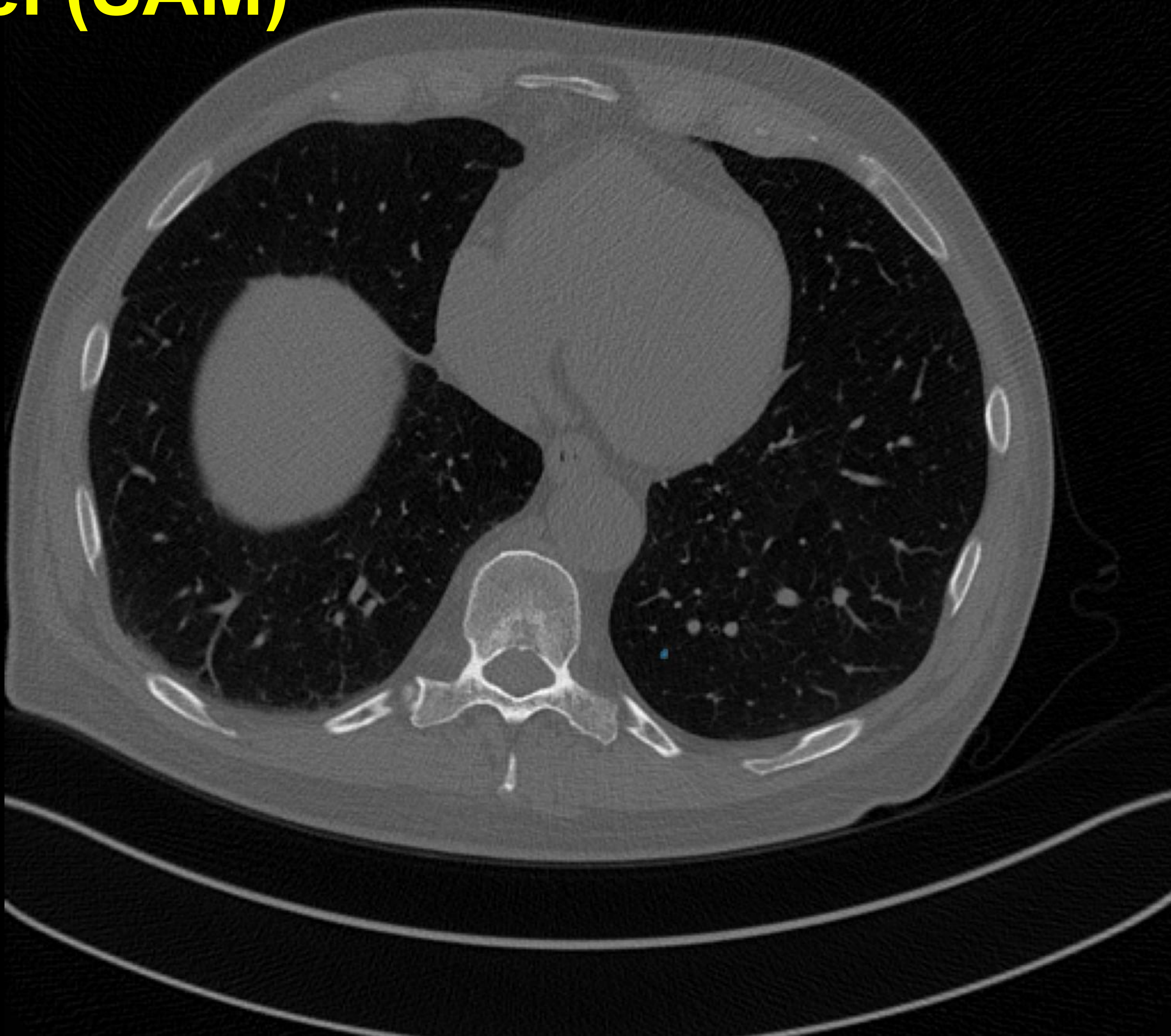

[1]Kirillov, Alexander, Eric Mintun, Nikhila Ravi, Hanzi Mao, Chloe Rolland, Laura Gustafson, Tete Xiao, et al. 2023. “Segment Anything.” arXiv.
[2]Ma, Jun, Yuting He, Feifei Li, Lin Han, Chenyu You, and Bo Wang. 2024. “Segment Anything in Medical Images.” *Nature Communications* 15 (1): 654.

Segment RMSE (SRMSE)

- Assume *S* segments from SAM for a given patient volume.
- Represent each segment by a binary mask volume $m^{(s)} \in \{0, 1\}^N$ with *N* being the number of voxels.
- Define the segment-wise root mean square error between two images *x* and *y*, and segment *s*:

$$\mathrm{SRMSE}(x, y; s) = \sqrt{\frac{\sum_{n=1}^{N} m_n^{(s)} (x_n - y_n)^2}{\sum_{n=1}^{N} m_n^{(s)}}}$$

- Using the set of all SRMSEs, define

$$\mathrm{MeanSRMSE}(x, y) = \frac{1}{S} \sum_s \mathrm{SRMSE}(x, y; s)$$

$$\mathrm{MaxSRMSE}(x, y) = \max_s \mathrm{SRMSE}(x, y; s)$$

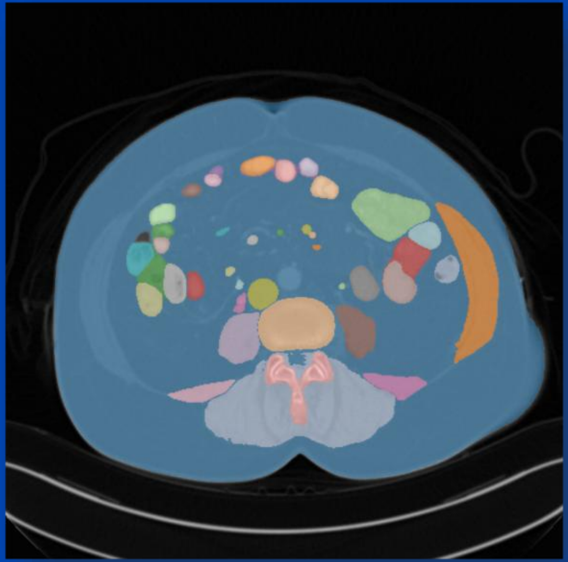

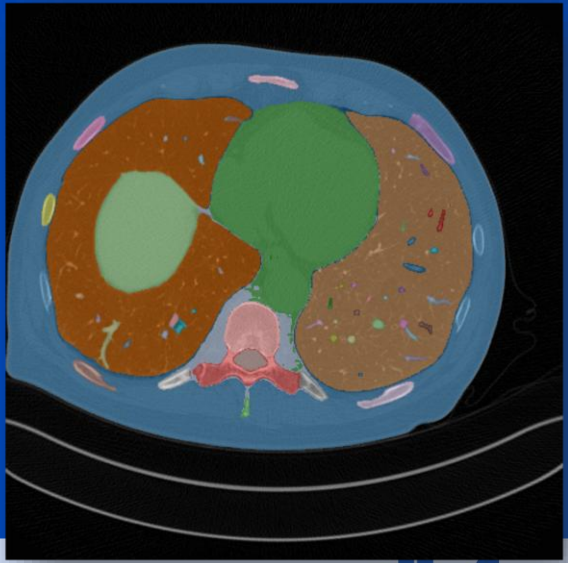

Experiments

- Evaluate the proposed metric on synthetic datasets where the amount of removed structures is known.
- Utilize three datasets from the Medical Decathlon[1], a collection of ten medical image segmentation tasks with ground truth annotations.

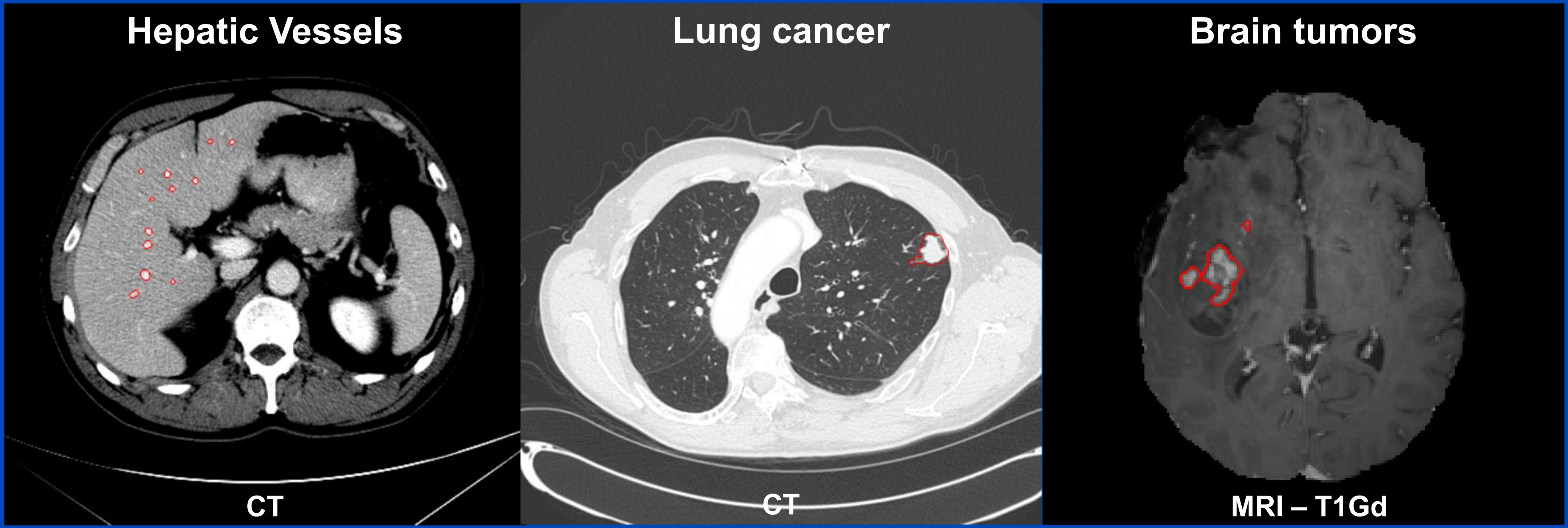

[1]Simpson, Amber L., Michela Antonelli, Spyridon Bakas, Michel Bilello, Keyvan Farahani, Bram van Ginneken, Annette Kopp-Schneider, et al. 2019. “A Large Annotated Medical Image Dataset for the Development and Evaluation of Segmentation Algorithms.” arXiv.

dkfz.

Hepatic Vessels

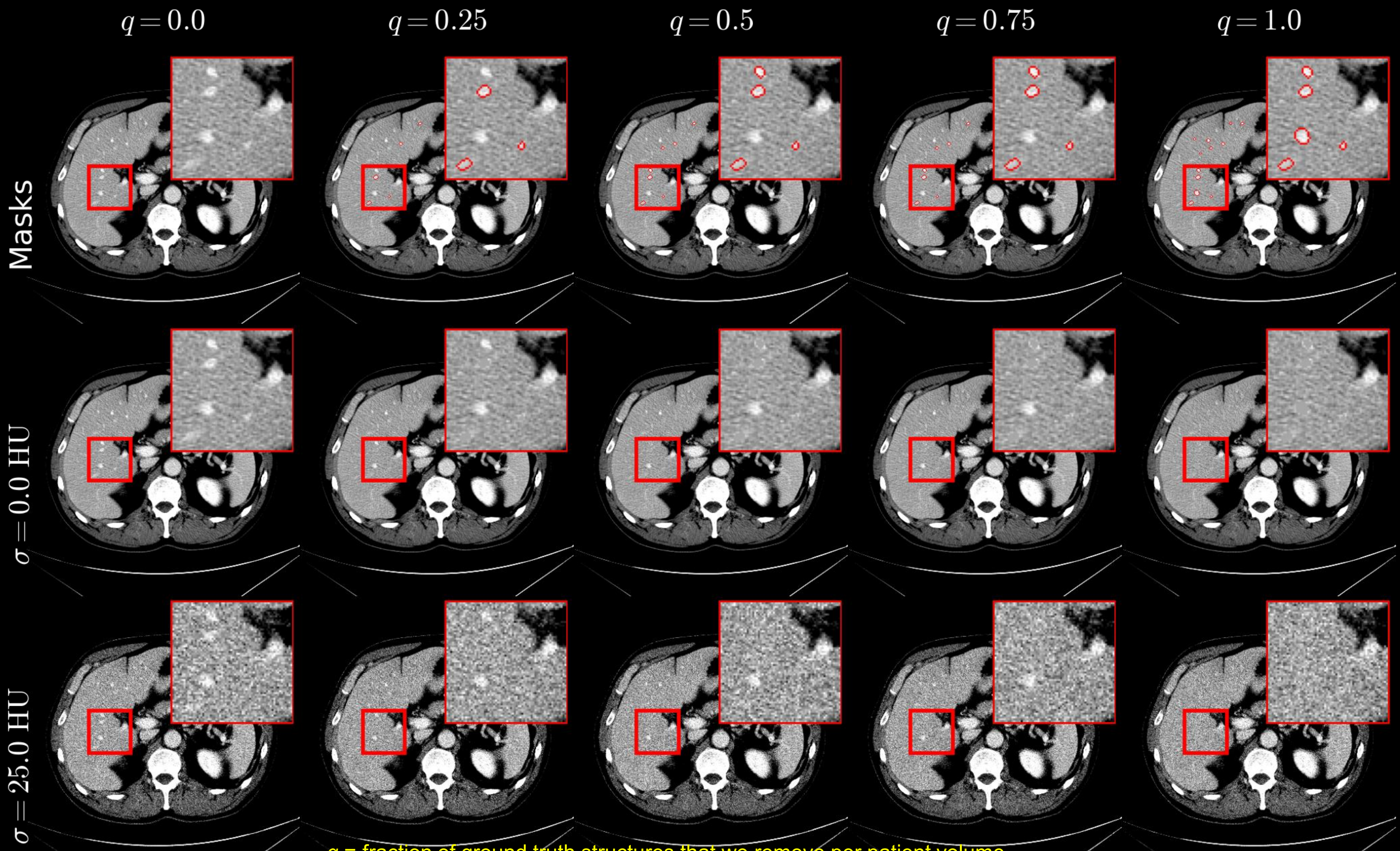

q = fraction of ground truth structures that we remove per patient volume
σ = standard deviation of additional Gaussian noise that is added to the images

Lung Cancer

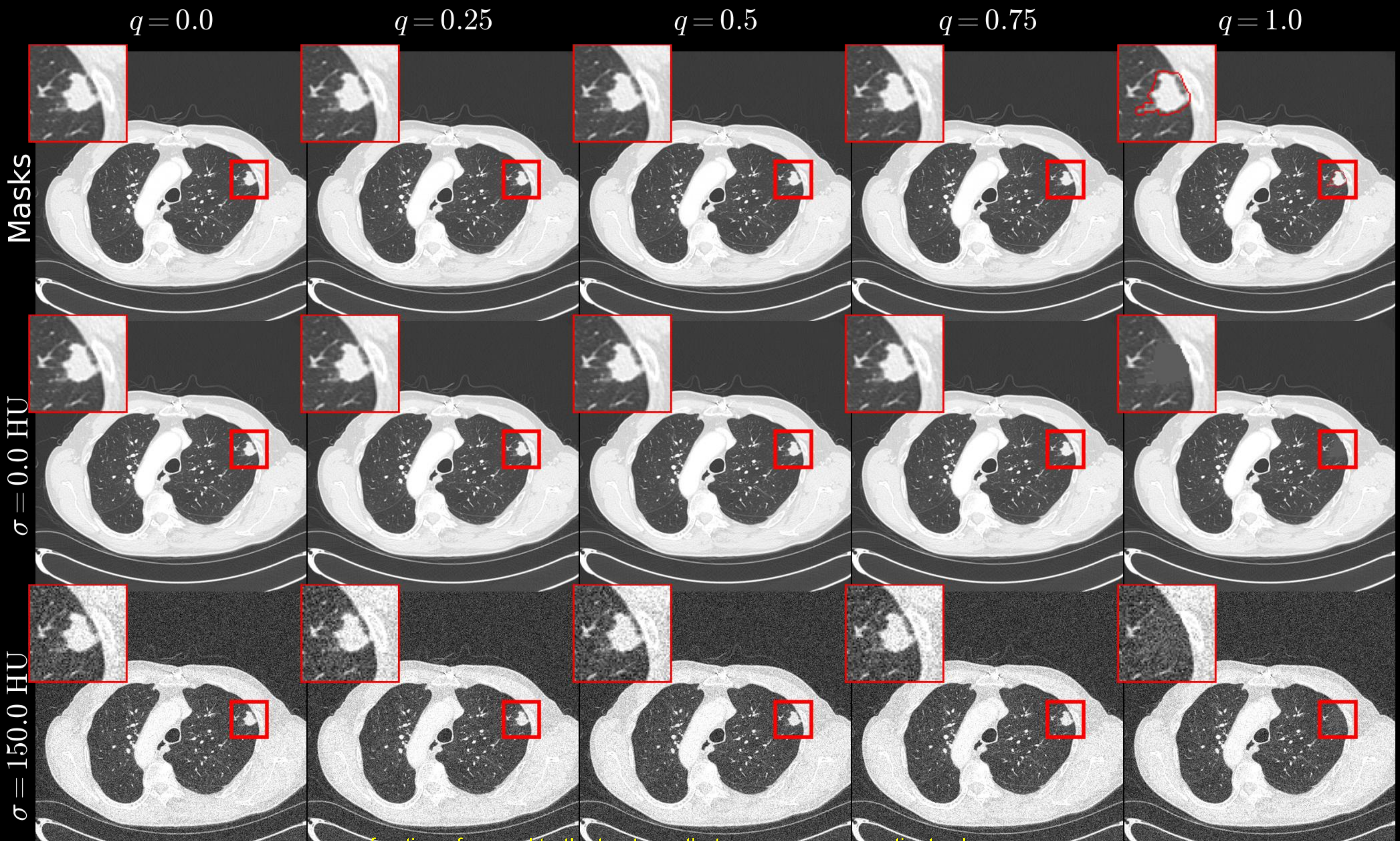

q = fraction of ground truth structures that we remove per patient volume
σ = standard deviation of additional Gaussian noise that is added to the images

Brain Tumor

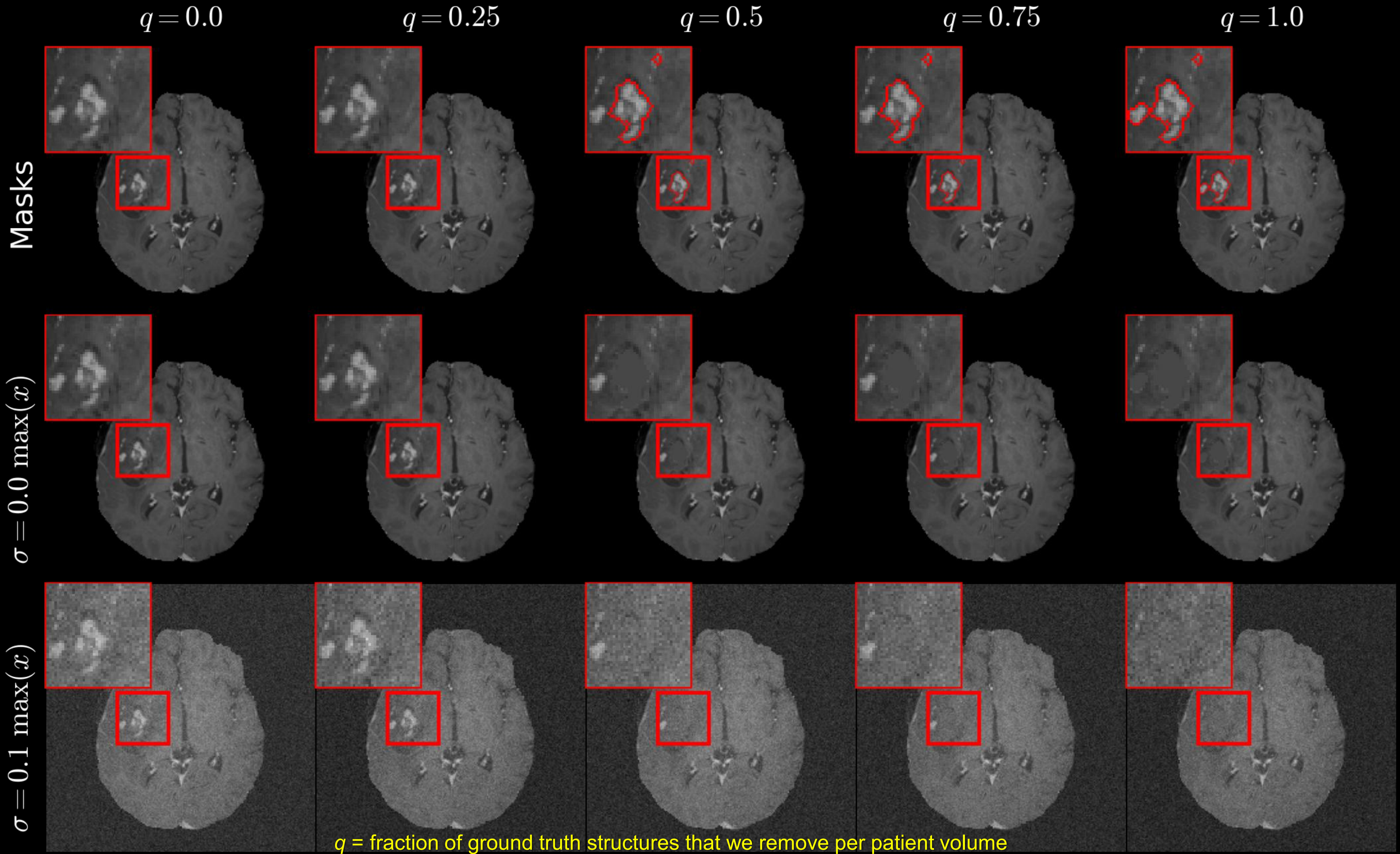

q = fraction of ground truth structures that we remove per patient volume
σ = standard deviation of additional Gaussian noise that is added to the images

Results: True Positive Fraction (Recall)

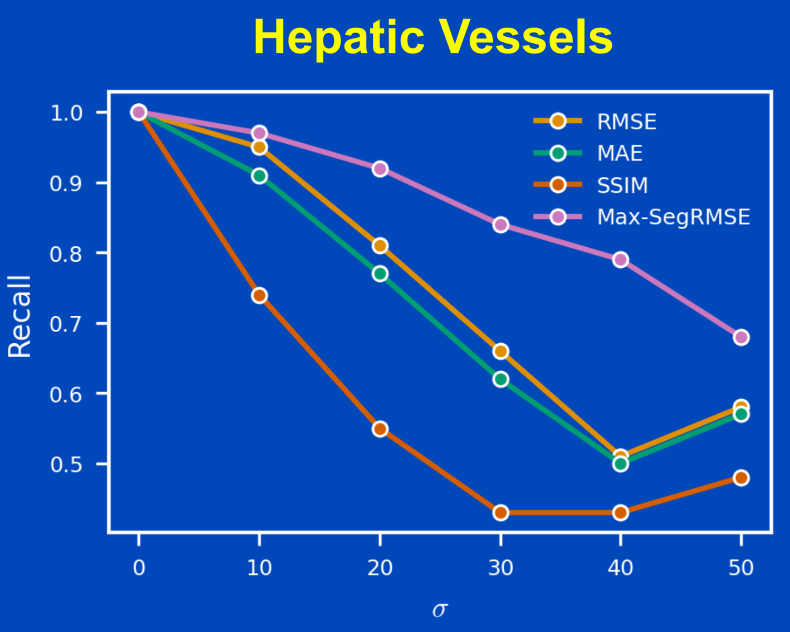

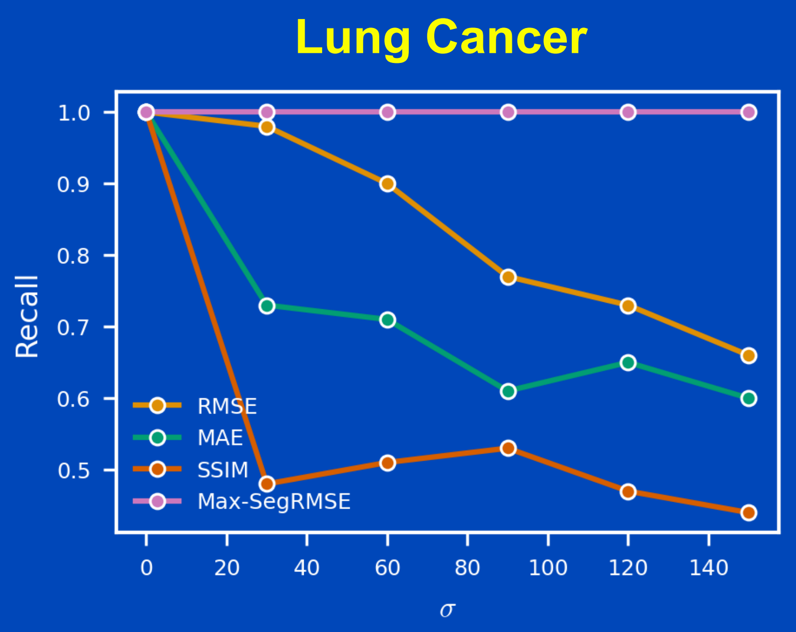

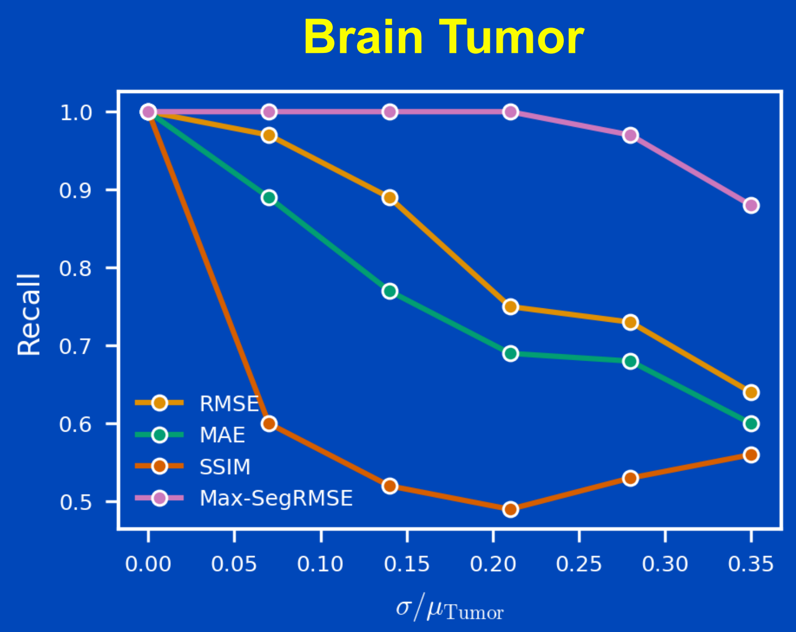

The plots show the likelihood that a metric correctly detects that images with *q* = 0.1 are worse (have more structures removed) than those with *q* = 0.

Note that *q* = 0.1 corresponds to about 0.007% to 0.03% modified voxels.

Risk-based tube current modulation

AI TO DRIVE TCM

RiskTCM

Remainder 0.12
Bone surface 0.01
Brain 0.01
Breast 0.12
Colon 0.12
Red Bone Marrow 0.12
Salivary glands 0.01
Esophagus 0.04
Liver 0.04
Lung 0.12
Skin 0.01
Stomach 0.12
Gonads 0.08
Thyroid 0.04
Bladder 0.04

- Risk-minimizing tube current modulation
- Weights the dose according to organ sensitivity.
- Finds $I(\alpha)$ that minimizes D_{eff} while keeping image noise constant.

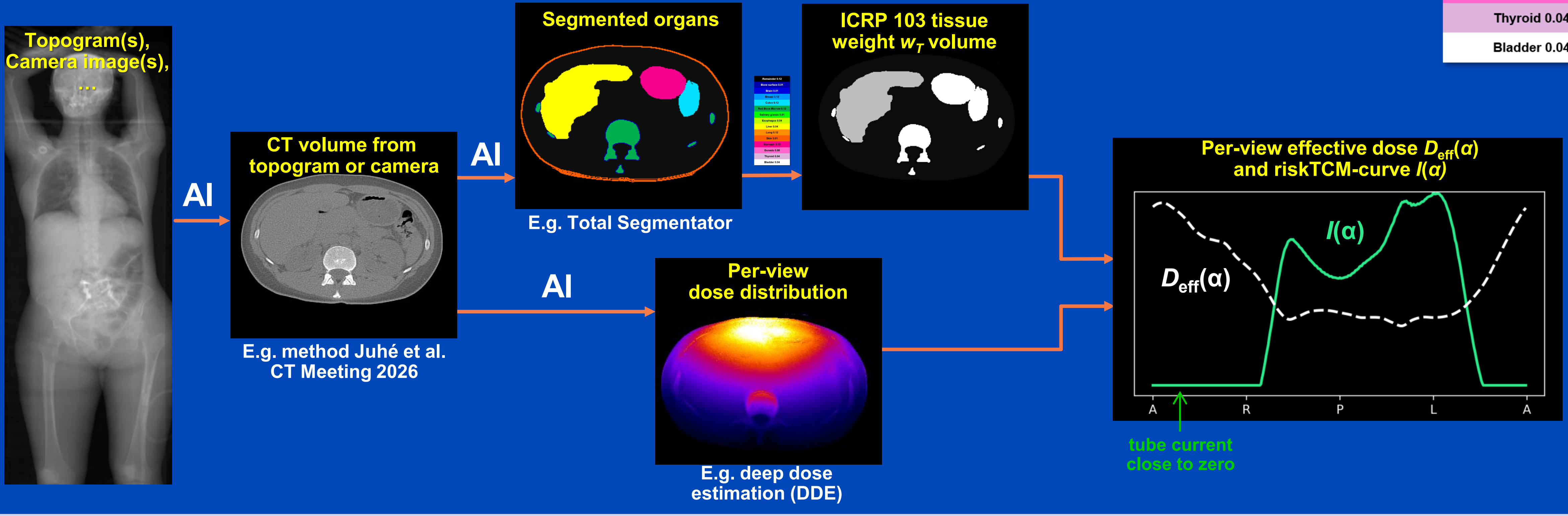

L. Klein, C. Liu, J. Steidel, L. Enzmann, M. Knaup, S. Sawall, A. Maier, M. Lell, J. Maier, and M. Kachelrieß. Patient-specific radiation risk-based tube current modulation for diagnostic CT. Med. Phys. 49(7):4391-4403, July 2022. *This paper received the Sylvia&Moses Greenfield Award for the best scientific paper on imaging in Medical Physics in 2022.*

dkfz.

Deep Dose Estimation (DDE)

- Combine fast and accurate CT dose estimation using a deep convolutional neural network.
- Train the network to reproduce MC [redacted] ven the CT image and a first-ord [redacted]

1 second
per tomographic data set

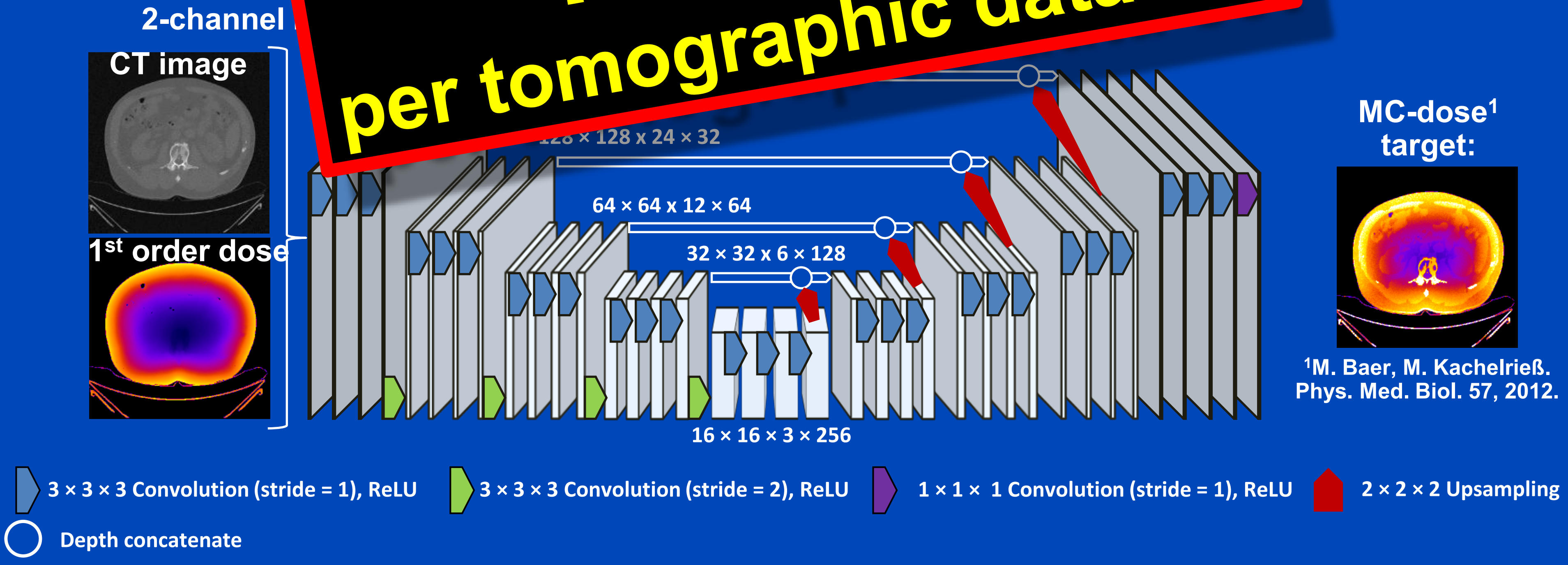

[1]M. Baer, M. Kachelrieß. Phys. Med. Biol. 57, 2012.

J. Maier, L. Klein, E. Eulig, S. Sawall, and M. Kachelrieß. Real-time estimation of patient-specific dose distributions for medical CT using the deep dose estimation. Med. Phys. 49(4):2259-2269, April 2022. *Best Paper within Machine Learning at ECR 2019!*

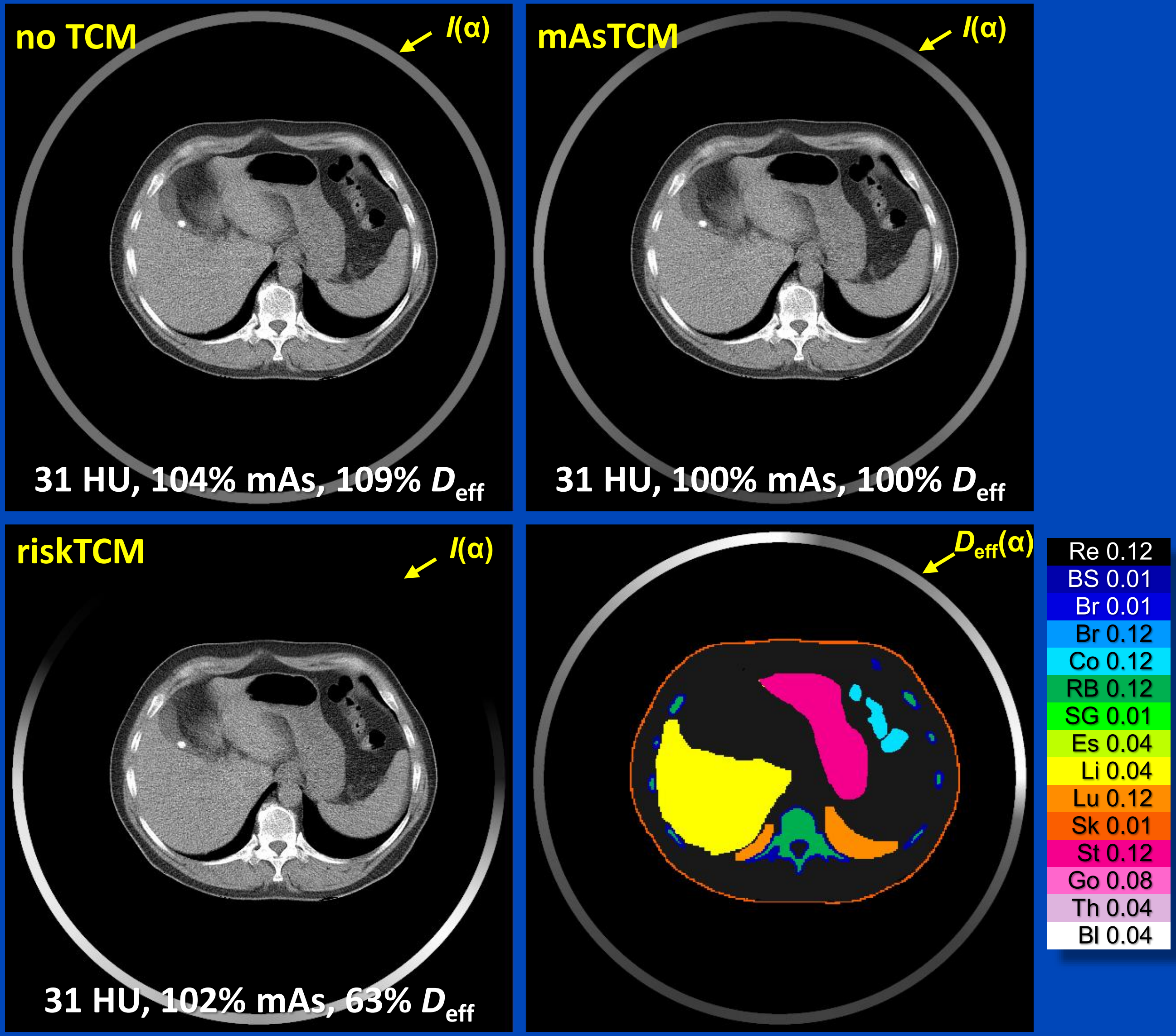

C = 25 HU, W = 400 HU

Conclusions on riskTCM

- Risk-specific TCM minimizes the patient risk.
- With Deff as a risk model riskTCM can reduce risk by up to 30%, compared with the gold standard mAsTCM.
- Other risk models, in particular age-, weight- and sex-specific models, can be used with riskTCM as well.
- Note:
  - mAsTCM = good for the x-ray tube
  - riskTCM = good for the patient

It is up to the vendors to take action!

L. Klein, C. Liu, J. Steidel, L. Enzmann, M. Knaup, S. Sawall, A. Maier, M. Lell, J. Maier, and M. Kachelrieß. Patient-specific radiation risk-based tube current modulation for diagnostic CT. Med. Phys. 49(7):4391-4403, July 2022. *This paper received the Sylvia&Moses Greenfield Award for the best scientific paper on imaging in Medical Physics in 2022.*

Thank You!

The 10th International Conference on Image Formation in X-Ray Computed Tomography

This presentation will soon be available at www.dkfz.de/ct.

Parts of the reconstruction software were provided by RayConStruct® GmbH, Nürnberg, Germany.